Effects of Variation of Temperature on the Radiative Recombination in a Thin film of Gallium Antimonide (GaSb)

By

Naol Mendera Fufa

September 2018

Effects of Variation of Temperature on the Radiative Recombination in a Thin film of Gallium Antimonide (GaSb)

By
Naol Mendera Fufa

A Thesis Submitted to the Department of Applied Physics program

Presented in Partial Fulfilment of Requirements of the Degree for

Masters of Science

in Applied Physics (Material Physics)

School of Applied Natural Sciences Office of Graduate Studies

Adama Science and Technology University

Advisor

Dr. Megersa Wodajo Shura

Adama, Ethiopia

September 2018

ADAMA SCIENCE AND TECHNOLOGY UNIVERSITY

POSTGRADUATE PROGRAM

SCHOOL OF APPLIED NATURAL SCIENCE

APPLIED PHYSICS PROGRAM

As thesis research advisor, I hereby certify that I have read and evaluated this thesis entitled: **"Effects of Variation of Temperature on the Radiative Recombination in a Thin film of Gallium Antimonide (GaSb)**" prepared under my guidance by **Naol Mendera**. I recommend that it can be submitted as fulfilling the thesis requirement.

Dr. Megersa Wodajo _____ _____

Advisor Signature Date

As members of the Board of Examiners of the M.Sc. thesis Open Defense Examination, we certify that we have read and evaluated the thesis work prepared by **Naol Mendera** and examined the candidate. We recommended that the thesis be accepted as fulfilling the thesis requirement for the Degree of Master of Science in Physics.

_____ _____ _____

Chairperson Signature Date

_____ _____ _____

Internal Examiner Signature Date

_____ _____ _____

External Examiner Signature Date

Declaration and Statement of the Candidate

I solemnly declare that this thesis work is not submitted to any other institution anywhere for the award of any academic degree, diploma, or certificate. Brief quotations from this thesis are allowable without special permission provided that accurate acknowledgement of source is made. Requests for permission for extended quotation from or reproduction of this manuscript in whole or in part may be granted by the head of major department or the Dean of the School of Graduate Studies when in his or her judgment the proposed use of the material is in the interests of scholarship. In all other instances, however, permission must be obtained from the author.

Name of candidate: Naol Mendera Signature: _____

Place: Adama Science and Technology University, Adama

Date of Submission: September 2018

ACKNOWLEDGEMENTS

First of all, I would like to thanks to the almighty God who gave me this chance and the successful accomplishment of my study. Next, I would like to thank my advisor, Dr. Megersa Wodajo for his constructive comments and endless support from the beginning to the end of my study in the program of Applied Physics. I am also grateful for his insightful lectures that I took advantage of writing this thesis. I would like to thank the Nelson Mandela Metropolitan University, South Africa for their giving some practical measured parameters of GaSb samples. I respectfully thank ASTU and Department of Applied Physics Program for giving me the sponsorship to study my M.Sc. Finally, I would like to express thanks from bottom of my heart to all my family Members, particularly, my brother, Urgesa Mendera for his love, and continues support. Last but not least, my heartfelt gratitude goes to fellow friends and colleagues. They deserve special thanks for their valuable contributions and encouragement.

Table of Contents

Contents **pages**

List of figures

Figures pages

List of Symbols and Abbreviations

T	Temperature (K)
k_B	Boltzmann's constant $\frac{J}{K}$
E_g	Energy band gap (eV)
$E_g(0)$	Band gap energy at absolute zero on the Kelvin (eV)
$E_g(T)$	Band gap energy at any temperature (eV)
E_{ph}	Energy of photon(eV)
eV	Electrovolt
GaSb	Gallium Antimonide
E_C, E_V	Energy of conduction band and valance band (eV)
α	Absorption coefficient (cm^{-1})
β	Beta (K)
λ	Photon Wavelength (nm)
c	Speed of light $(^m/_s)$
h	Plank's constant(Js)
$\hbar$	Reduced plank's constant(Js)
EHP	Electron hole pairs
K	Kelvin
v	Photon frequency s^{-1}
k	Wave number
C_R	Carriers radiative capture coefficient (cm^3s^{-1})
E_i	Intrinsic Fermi energy(eV)
E_F	Fermi energy (eV)
E_{BF}	Bulk Fermi energy (eV)
E_{SF}	Surface Fermi energy (eV)
E_S	Energy surface (eV)
Φ_0	Incident photon flux density $(cm^{-2}s^{-1})$
$\Delta\Phi$	Absorbed photon flux density $(cm^{-2}s^{-1})$
Φ_s	Photon flux density entering the illuminated surface
Δx	Change in thickness(depth) (m)
b	Thickness of layer (m)
Δt	Time interval (s)
A	Area (cm^{-2})
l	Length of layer (cm)

w	Width of layer (cm)
ΔN_{ph}	Number of photon absorbed
G_{th}	Thermal equilibrium Generation rate Electron and hole ($cm^{-3}s^{-1}$)
G_0	Photon absorption rate ($cm^{-3}s^{-1}$)
G	Total generation rate ($cm^{-3}s^{-1}$)
R	Total recombination rate ($cm^{-3}s^{-1}$)
U	Net recombination rate ($cm^{-3}s^{-1}$)
U_R	Radiative recombination rate ($cm^{-3}s^{-1}$)
τ_n, τ_p	Lifetime for electron and holes (s)
m_n^*, m_p^*	electron and hole Effective mass (kg)
m_0	Rest mass of the electron (kg)
ε_0	Permittivity of free space $\frac{c^2}{Jm}$
e	Elementary charge (c)
n_i	Intrinsic carrier density (cm^{-3})
n_0, p_0	Thermal equilibrium concentration of electron and hole (cm^{-3})
n, p	Non-thermal equilibrium concentration of electron and hole (cm^{-3})
$\delta n, \delta p$	Excess charge carrier concentration for electron and hole density (cm^{-3})
N_C, N_V	Effective density in the conduction and valence band (cm^{-3})
N_a	Acceptor concentration (cm^{-3})
n	Index of refraction
R	Reflectivity
x	Depth below the illuminated surface
x_p	Penetration depth of the light (m)
k_∞	Dielectric constant
π	Pi
τ_R	Radiative excess carrier lifetime(s)
τ_k	Time constant of the radiative recombination (s)
τ_g	Excess generation carrier lifetime (s)
v_{th}	Thermal velocity of the electrons ($^m/_s$)
α_R	Carrier capture cross section

Abstract

In this study, the effects of temperature on the radiative recombination of Gallium Antimonide (GaSb) thin film semiconductor are investigated. First, using the illumination mechanism, the photon absorption rate as a function of the depth below the illuminated surface in both the bulk and the thin films of GaSb were determined at different temperature. Then, the depths below illuminated surface dependence of the low injection level thermal equilibrium carrier concentrations in a thin film of Gallium Antimonide (GaSb) at different temperature were investigated by considering the variation of the energy bending at the surface. Finally, using the steady state condition of the free carrier's generation recombination mechanism, the radiative excess carrier lifetime of the photo-generated free carriers is described in both thin films and the bulk material as function of the depth below the illuminated surface at different temperatures and injection levels. The obtained result indicates that, photon absorption rate and the free carrier's generation rate in general increases with decreasing the thickness of the thin films and the variation of the absorption rate with the thicknesses of the samples is high for high temperatures. The photo-response of the thin film semiconductor is in general found to be dominated by the property of the surface depletion layers of the material and hence extremely higher than the photo response of the deep bulk.

Chapter 1 : Introduction

1.1 Background

The history of semiconductors is long and complicated. Obviously, one cannot expect it to fit one short paper. According to G. Busch the term “semiconducting” was used for the first time by Alessandro Volta in 1782. The first documented observation of a semiconductor effect is that of Michael Faraday (1833), who noticed that the resistance of silver sulfide decreased with temperature, which was different than the dependence observed in metals. An extensive quantitative analysis of the temperature dependence of the electrical conductivity of Ag_2S and Cu_2S was published in 1851 by Johann Hittorf. For some years to come the history of semiconductors focused around two important properties this mean rectification of metal-semiconductor junction and sensitivity of semiconductors to light [1].

Semiconductors are widely used for emission and detection of radiation. The first, report on light emitted by a semiconductor appeared in 1907 in a note by H. J. Round. Fundamental work in this area was conducted, among other, by Losev [2]. The first semiconductor lasers were developed around 1962 by four American research teams. Further research in this area went in two directions, i.e., wider spectrum of materials to obtain wider wavelength range and concepts of new device structures. Herbert Kroemer and Zhores Alferov have independently come up with the idea that semiconductor lasers should be built on heterostructures. Zhores Alferov was a member of the team that created the first Soviet p-n junction transistor in 1953. He was directly involved in research aimed at development of specialized semiconductor devices for Russian nuclear submarines. The matter was of such importance for the Soviet authorities that he used to receive phone calls from very high government officials who wanted the work done faster. To fulfil those requests Alferov had to move to the lab and literally live there. Later he worked on power devices and became familiar with p-I-n and p-n-n structures. When the first report on semiconductor lasers appeared, he realized that double heterostructures of the p-I-n type should be used in these devices. He obtained the first practical heterostructures devices and the first heterostructures laser [3].

Almost all of today technology involves the use of semiconductors, with the most significant aspect being the integrated circuit [4]. Temperature has been proved to be a valuable tool for studying the influence on the electronic properties of semiconductors, bulk crystals, or two dimensional systems, thus, we have studied effect of the temperature on some properties of semiconductors, that is, the fact that the conductivity in semiconductors increases with increasing temperature, whereas the conductivity in metals decreases with increasing temperature [5, 6]. Researchers who reported that the temperature dependence of the excess carrier life time of semiconductors, as temperature increases, lifetime due to the radiative recombination decreases sharply [7, 8]. Semiconductors are the foundation of modern electronics and optoelectronic. Electronic and optoelectronic components such as transistors and laser diodes are made of semiconductor materials, and they are crucial to almost any electronic and optoelectronic device. Semiconductors can be either elemental or compound semiconductors. The elemental semiconductors are silicon and germanium. There are dozens of different compound semiconductors being used in industry and studied in the field of materials science [9].

Semiconductor materials exhibit a number of useful unique properties related to their electronic structure. They can be fabricated to be in bulk or in thin film forms. Thin films are thin material layers ranging from fractions of a nanometre to several micro meters in thickness. The thickness is typically less than several microns. Thin films are also regarded as two dimensional materials fabricated by the process of condensation of atoms, molecules or ions. This is what makes them to have unique properties significantly different from their corresponding bulk materials. These unique properties are as a result of the changes that occur in their physical dimensions, geometry and microstructure [10, 11]. Semiconductors are materials whose energy gap lies precisely between that of insulators and metals. The determining factor for conduction in semiconductors is the nature of energy gap between the valence band and the conduction band.

The III–V compound semiconductor Gallium Antimonide (GaSb) has in recent years attracted much attention as an important material for infrared (IR) optoelectronic and suitable for fabricating high-frequency electronic device [12, 13]. The photo response of this material makes it very useful in the design of a variety of device architectures, including photo detectors, resonant tunnelling structures and other quantum devices.

The performance of the material is depends on the lifetime of free charge carriers generated by the interaction of light with the material, referred to as the excess carrier lifetime. Minority carrier lifetime is one of the most important parameters which has a decisive effect on the performance of material based on excess carriers generated by the interaction of light with the material, referred to as the excess carrier lifetime. Many researchers [14, 15, 16] reported that the lifetime of the radiative recombination mechanism of semiconductor material decreases with increase in doping concentration, injection level, and majority carrier density. Shura et al [17] measured the injection level dependence of the excess carrier recombination lifetime on the p-type Gallium Antimonide thin films (GaSb) semiconductor, hence the result obtained that the lifetime values decreases with increase in injection levels. In thin films there are deviations from the properties of the corresponding bulk materials that arise because of their small thickness, large surface- to- volume ratio and their unique physical structure which is a direct consequence of the growth process. A semiconductor material is said to be in thin film form only when it is built up as a thin layer on a solid support called substrate by a controlled condensation of the individual atomic, molecular, or ionic species [18].

Thin films are widely used in a large number of solid state devices. Some of these applications include photoconduction which is the change in the electrical conductivity of a substance, as a result of absorbing electromagnetic radiation [19]. In recent years, polycrystalline thin-film solar cells have been of much interest because of their potential in the reduction of weight and cost. This is even more so when solar cells are to be considered for multi-kilowatt power systems. However, most of the work has been concentrated on individual cells. The conventional assembly of these cells into large arrays would be, to a certain degree, similar to that for single-crystal cells. In these assembly techniques lies the major portion of the cost and weight for the final power system. To realize more fully the potentials of thin-film cells, techniques should be developed where by large arrays containing numerous interconnected cells can be produced automatically, thus eliminating the separate, manual operations of cell mounting and interconnection also eliminating the need for a separate cell-support array member. This is quite analogous to the increasing application of integrated microelectronic circuits today [20].

In general, in previous using the results from Hall Effect measurements along with the relations describing the lifetimes of the excess minority carriers in the semiconductors, the theoretical values of the excess carrier lifetimes in the materials were studied [21, 22]. But, Investigation of the optical and electrical behavior of some semiconductors such thin film of Gallium Antimonide (GaSb) with depth below illuminated surface has not been much study, at least not experimentally. The importance of such research becomes obvious due to the variation of some of those properties of thin film Gallium Antimonide (GaSb) with depth below the illuminated surface.

1.2 Objectives of the study

The general objective of this work is to study the effects of Variation of temperatures on the Radiative Recombination in a Thin film of Gallium Antimonide (GaSb) Semiconductor. The specific objectives of the study is:

- to determine the photon absorption effect in both thin film and bulk Gallium Antimonide Semiconductor,
- to describe the variation of Energy bending with depth below the illuminated surface at different temperatures,
- to study the thermal equilibrium carrier concentration as function of depth under the surface of semiconductor at different temperatures,
- to determine the radiative excess carrier lifetime under different conditions.

1.3 Thesis Outlines

This thesis organized into five chapters. **Chapter two** includes review of related literatures. It is contains five sub sections. It deals with the theory of energy bands in solids, thermal equilibrium properties of semiconductors, the near surface region at thermal equilibrium, photon absorption in semiconductors, optical generation and recombination of excess carrier photo-response of semiconductors. **Chapter three** presents the overall methodology by which important data is collected and analysed. **Chapter four** covers the results and discussion of the study. **Chapter five** gives the conclusions of entire parts of this work and describes the results obtained in chapter four.

Chapter 2 : Literature Review

2.1 Energy bands in solids

Band structures are a representation of the allowed electronic energy levels of solid materials and are used to better inform their electrical properties. A band structure is a two dimensional representation of the energies of the crystal orbitals in a crystalline material. A band structure can quickly reveal whether a material is metallic, semi-metallic, or insulating, and for those materials with bandgaps whether they are direct or indirect as well as the magnitude of the gap. Additionally, the curvature of the bands can reflect the carrier mobility through those bands [23]. The band gap is an energy range where no electronic states are present.

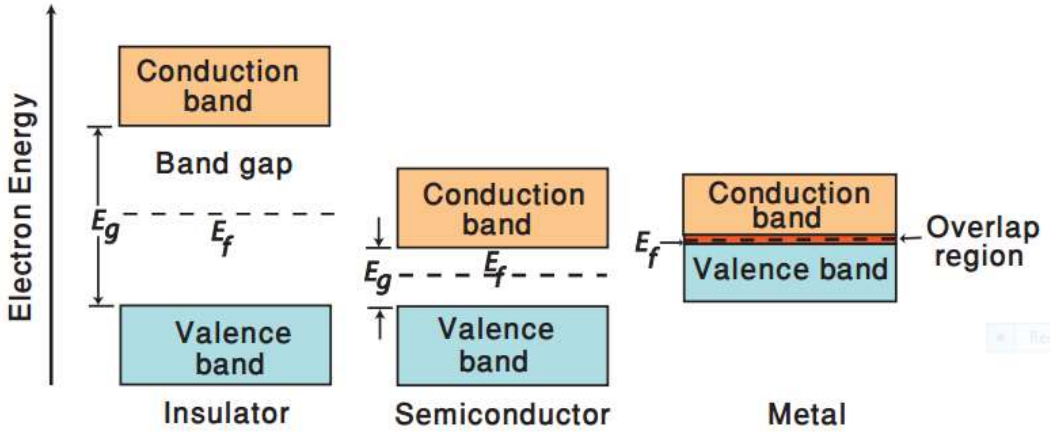

Figure 2-1: Simplified diagram of the electronic band structure of insulators, semiconductors and metals. The position of the fermi level is when the sample is at absolute zero temperature (0 K) [24].

In conductors (i.e. metals) as shown in Figure 2-1, the conduction band is either partially filled or overlaps the valence band so that there is no band-gap. This causes the uppermost electrons in the partially filled band or electrons at the top of the valence band to move to the next higher available energy level when they gain kinetic energy. Through this, current conduction readily occurs in conductors. In semiconductors, the bonds between neighbouring atoms are only moderately strong. When thermal vibrations occur they break some of the bonds and free electrons along with free holes are produced. That is, why the band gap of a semiconductor is not as large as that of an insulator. Therefore, some electrons will be able to move from the valence band to the conduction band leaving holes in the valence band. If an electric field is applied, then both the electrons in the conduction band and the holes in the valence band will gain kinetic energy and conduct electricity. The valence electrons

form strong bonds between neighbouring atoms in insulators. These strong bonds are difficult to break. This means that there are no free electrons to participate in current conduction. This causes the band gap in an insulator to be large. When we consider the band gap in an insulator, thermal energy or any external applied electric field cannot raise the uppermost electron in the valence band to the conduction band [25].

Fermi level is an important consequence of band theory, the highest occupied quantum state of electrons at absolute zero temperature. The position of the Fermi level relative to the conduction band is an important parameter that contributes to determine the electrical properties of a particular material. The position of the Fermi level position is also indicated in Figure 2-1. For a semiconductor, the electrical resistivity lies between a conductor and an insulator. An externally applied electrical field may change the semiconductor's resistivity. In conductors, current is carried by electrons, whereas in semiconductors, current is carried by the flow of electrons or positively charged holes [24]. In a crystalline solid, the energy difference between the top of valance band (E_V) and the bottom of conduction band (E_C) is defined as the band-gap energy (E_g). The band-gap energy of a semiconductor defines its optical absorption threshold for the photoelectric effect. That is, generation of electric charge-carrier from light absorption only occurs with photons with energies greater or equal to the band gap, ($h\upsilon \geq E_g$), where E_g is the energy band gap of the given semiconductor, h the Planck's constant and υ, the frequency of the absorbed photon by the semiconductor. When supra-band-gap light is absorbed by a semiconductor, charges move between the valence and conduction bands [26, 27]. When a semiconductor is illuminated by a photon of energy greater than its energy band gap ($h\upsilon > E_g$), electron-hole pairs are generated in the semiconductor. The photo-response of the semiconductor can be described through the current produced due to the electron-hole pairs produced in the process. Hence, the amount of current produced by these charge carriers is also affected by the effective lifetime of the carriers. The band gap energy $E_g = E_C - E_V$, is perhaps the most important in semiconductor physics. A contraction of the crystal lattice with decreasing temperature usually leads to a strengthening of the interatomic bonds and an associated increase in the band gap energy. The first empirical relation for the band gap shift with temperature was developed by Varshni et al [28, 29]. The

temperature dependence of the energy band-gap, $E_g(T)$ has been experimentally determined yielding the following expression as a function of the temperature, T.

$$E_g(T) = E_g(0) - \frac{\alpha T^2}{T + \beta}. \tag{2-1}$$

where $\alpha = 3.78 \times 10^{-4}$ eV/Kand $\beta = 94\ K$ are constants chosen to obtain the best fit to experimental data and $E_g(0)$ is 0.813 eV the limiting value of the band at zero Kelvin.

Therefore, Gallium Antimonide's basic band structure shows a direct energy gap between the valance band maximum and the conduction band minimum direct gap semiconductors eliminate the need for phonons to allow the transition of the electron from the valance band to the conduction band [30]. The basic difference between direct gap and indirect gap transitions is that, when the conduction band minimum and the valence band maximum occur at different value of k, the material is said to be indirect band-gap material. On the other hand Electronic transitions between the two bands, with no change in crystal momentum is said to be direct band gap [31].

2.2 Thermal equilibrium properties of semiconductors

In this section, the description of some common properties of semiconductor materials like the energies of the charge carriers and the free charge carrier concentrations will be discussed.

2.2.1 Thermal equilibrium carrier concentration

The concentrations of electrons and holes in a semiconductor are determined by many factors including the bandgap and band structure of the semiconductor, the types and concentrations of the impurities doped in the semiconductor, temperature and any external disturbances to the semiconductor [32]. The term equilibrium is used to describe the unperturbed state of a system, to which no external voltage, illumination, mechanical stress, or other perturbing forces are applied. Therefore, thermal equilibrium concentration of electron and hole in conduction and valance bands are independent of time. In thermal equilibrium electron-hole pairs are constantly being formed and destroyed. For a non- illuminated semiconductor in thermal equilibrium, the concentration of electrons in the conduction band is $n = n_0$ and holes in the valence band $p = p_0$. The thermal equilibrium electron concentration, n_0 in the conduction

band and thermal equilibrium hole concentration, p_0 in the valence band for the non-degenerate semiconductor case can be simplified to [33, 34]:

$$n_0 = N_C \, exp\left(-\frac{E_C - E_F}{k_B T}\right), \tag{2-2}$$

Where

$$N_C = 2\left(\frac{2\pi m_n^* k_B T}{h^2}\right)^{3/2}. \tag{2-3}$$

N_C is the the effective density of the conduction band states and m_n^* is effective mass of electrons in the conduction band. The density of the hole carriers, p_0 in the valence band can be derived also for non-degenerate case as:

$$p_0 = N_V \, exp\left(-\frac{E_F - E_V}{k_B T}\right), \tag{2-4}$$

where

$$N_V = 2\left(\frac{2\pi m_p^* k_B T}{h^2}\right)^{3/2}. \tag{2-5}$$

N_V is the effective density of the valence band states and m_p^* is the effective mass of holes in the valence band.

2.2.2 Intrinsic semiconductors

Pure semiconductors (i.e., semiconductors with no intentional doping) [35] or a perfect semiconductor crystal with no impurities or lattice defects is called an intrinsic semiconductor. A semiconductor may be considered as an intrinsic semiconductor if its thermally generated carrier density represented by n_i is much larger than the back ground doping or residual impurity densities. At $T = 0\ K$ an intrinsic semiconductor behaves like an insulator because the conduction band states are totally empty and the valence band states are completely filled. However, as the temperature increases, some of the electrons in the valence band states are excited into the conduction band states by thermal energy, leaving behind an equal number of holes in the valence band and the electron-hole pairs are produced. These electron-hole pairs (EHPs) are the only charge carriers in intrinsic material [36]. Therefore, the intrinsic carrier density increases with increasing temperature. Suppose that $\mathfrak{N}$ is the concentration of electron-hole pairs thermally generated in the respective bands and n_R is the concentration of electron-hole pairs annihilated after the generation, the free carrier

concentrations in the conduction and valence bands adjust for the intrinsic semiconductor to [8].

$$n_0 \approx \mathfrak{N} - n_R = n_i = p_0. \tag{2-6}$$

As we discussed in the above, the electron-hole pairs in an intrinsic semiconductor are generated by thermal excitation. Therefore, for intrinsic semiconductors with an energy band gap on the order of 1eV or higher, the intrinsic carrier density is usually very small at low temperatures below 100K. As a result, the resistivity for these intrinsic semiconductors is expected to be very high at low temperatures. Since the non-degenerate relations are obviously valid for an intrinsic semiconductor where the Fermi level, E_F is equal to the intrinsic level energy, E_i of the semiconductor,

$$n_i = N_V \exp\left(-\frac{E_i - E_V}{k_B T}\right) = N_C \exp\left(-\frac{E_C - E_i}{k_B T}\right), \tag{2-7}$$

The intrisic energy, E_i can be written from Eqns. (2-3) and (2-5) along with Eqn. (2-7) gives:

$$E_i = \left(\frac{E_V + E_C}{2}\right) + \frac{3}{4} k_B T \ln\left(\frac{m_p^*}{m_n^*}\right). \tag{2-8}$$

If E_V and E_C are known at a certain temperature, one can easily compute the values of n_i as function of temperature. The intrinsic concentration, n_i for free carriers the corresponding bands can be computed from Eqns. (2-2) and (2-4) above as:

$$n_i = \sqrt{p_0 n_0} = \sqrt{N_V N_C} \exp\left(-\frac{E_g}{2k_B T}\right). \tag{2-9}$$

Eqn.(2-9) is called the law of mass action [37].

2.2.3 Extrinsic semiconductor

In addition to the intrinsic carriers generated thermally, it is possible to create carriers in semiconductors by purposely introducing impurities into the crystal. This process, called doping, is the most common technique for varying the conductivity of semiconductors. By doping, a crystal can be altered so that it has a predominance of either electrons or holes. Thus there are two types of doped semiconductors, n-type (mostly electrons) and p -type (mostly holes). When a crystal is doped such that the equilibrium carrier concentration n_0 is different from the intrinsic carrier concentration n_i the material is said to be extrinsic. When impurities or lattice defects are introduced into an otherwise perfect crystal, additional levels are created in the energy band structure, usually within the band gap. This level is filled with electrons at

0 K, and very little thermal energy is required to excite these electrons to the conduction band. As the temperature is raised, these electrons are donated to the conduction band, and at about 100K all the donor atoms are ionized. This temperature range from $0k\ to\ 100k$ to is called the partially ionization region. Once, the donors are ionized, the conduction band electron concentration is $n_0 \sim N_d = 10^{16}\text{cm}^{-3}$, N_d Donor impurity atoms, since one electron is obtained for each donor atom. When every available extrinsic electron has been transferred to the conduction band, n_0 is virtually constant with temperature until the concentration of intrinsic carriers n_i becomes comparable to the extrinsic concentration N_d. Finally, at higher temperatures n_i is much greater than N_d, and the intrinsic carriers dominate. In most devices it is desirable to control the carrier concentration by doping rather than by thermal EHP generation. Thus, one usually dopes the material such that the extrinsic range extends beyond the highest temperature at which the device is to be used [38]. In the real case, there are many levels within the band-gap that can influence the concentration of electrons and holes in the conduction band and the valence band. One way to intentionally do so is to dope the material. Doping creates donor or acceptor levels, which are able to contribute an electron or a hole, respectively, to their corresponding conduction bands, as shown in Figure 2-2 below:

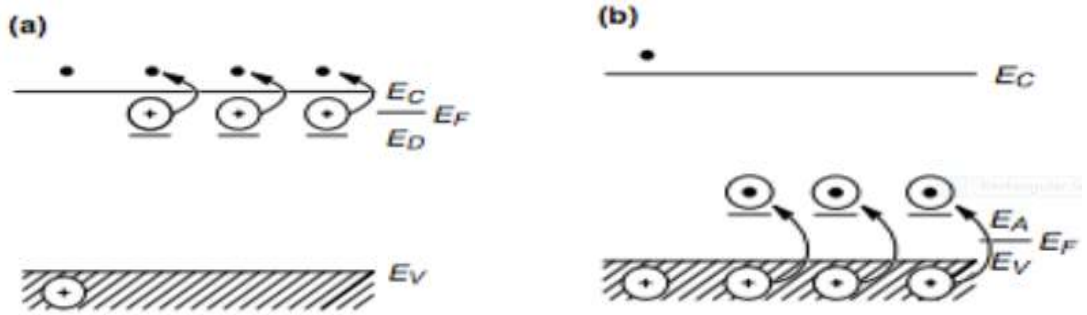

Figure 2-2: Diagram of n-type (a) and p-type (b) doped semiconductors. The donor energy level within the band-gap of (a) donates electrons to the conduction band. Similarly, the acceptor level of (b) accepts electrons and leaves conducting holes in the valence band [39].

The most important and unique feature of a semiconductor material lies in the fact that its electrical conductivity can be readily changed by many orders of magnitude by simply doping the semiconductor with shallow-donor or shallow-acceptor impurities. By incorporating the doping impurities into a semiconductor, the electron or hole density will increase with increasing shallow-donor or shallow-acceptor impurity concentrations. For example, electron or hole densities can increase from 10^{13}cm^{-3} to

more than 10^{20}cm^{-3} if a shallow-donor or shallow-acceptor impurity with an equal amount of impurity densities were added into a silicon crystal. In addition to the relatively shallow-level donors and acceptors, the substitution of other impurity atoms into a host semiconductor can give rise to deep-level states allowed states in the band gap more than a few tenths of an eV from either band edge. These are commonly referred to as traps or recombination-generation centers. Such centers are usually unintentional impurities, are not necessarily ionized at room temperature, and typically occur in concentrations far below the dopant concentration. The deep level centers can be donor-like (positively charged when empty and neutral when filled with an electron), acceptor-like (neutral when empty and negatively charged when filled with an electron), or may exhibit multiple charge states with associated multiple levels in forbidden gap.

As discussed above, adding donor or acceptor impurity atoms into semiconductor will change the distribution of electrons and holes in the material, and as a result, the position of Fermi energy will change. Eliminating N_C and N_V among Eqns.(2-2), (2-4) and (2-5) yields:

$$n_0 = N_C \exp\left(-\frac{E_C - E_F}{k_B T}\right) \qquad \text{and} \qquad p_0 = N_V \exp\left(-\frac{E_F - E_V}{k_B T}\right). \tag{2-10}$$

The law of mass action, Eqn. (2-9) allows one to calculate the minority carrier density in an extrinsic semiconductor when the majority carrier density is known.

$$\text{Minority carrier density} = \begin{cases} \dfrac{n_i^2}{p_0}, & \text{for p} - \text{type material,} \\ \dfrac{n_i^2}{n_0}, & \text{for n} - \text{type material.} \end{cases} \tag{2-11}$$

The thermal equilibrium extrinsic Fermi-level, E_F can also be described from Eqns. (2-2) and (2-4) in terms of E_i and the thermal equilibrium carrier concentrations as:

$$E_F = E_i - k_B T \ln\left(\frac{p_0}{n_i}\right) = E_i + k_B T \ln\left(\frac{n_0}{n_i}\right). \tag{2-12}$$

As the charge carrier concentrations change, the position of the extrinsic Fermi energy level varies within the band gap until the system reach thermal equilibrium. Eqn. (2-12) shows that E_F lies above E_i for n-type material ($n_i > p_0$) and below E_i for $p-$ type material ($n_i < p_0$) [40, 41].

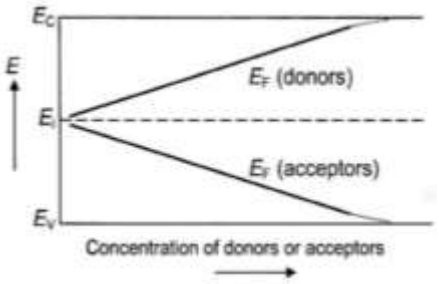

Figure 2-3: Variation of fermi energy with doping concentration.

Figure 2-3: shows the Fermi energy level as a function of donor concentration (n-type) and as a function of acceptor concentration (p-type). As the doping level increases the Fermi energy level moves closer to the valence band for the p-type material and closer to conduction band for the n-type material. Now, as doping concentration increases the Fermi energy level moves closer to the valence band because the material is p-type. If the Fermi energy level lies inside the conduction (or valence) band, the material is referred to as a degenerate semiconductor. The semiconductor becomes degenerate at high carrier concentrations above $p_0 = 10^{19}\text{cm}^{-3}$ [42].

2.3 The near surface region at thermal equilibrium

When an electric field (ε) is applied to the material, the band energies become a function of position. The variation of E_C and E_V with position is referred to as band bending [43]. The bulk of most isolated III-V semiconductors have three various regions of different carrier concentrations. This consists of a neutral region (with high thermal equilibrium majority carrier concentration), followed by a transition layer (with decreasing thermal equilibrium majority carrier concentration in moving towards the surface), and a depleted surface region of very low thermal equilibrium majority carrier concentration. In semiconductor physics, the depletion region, also called depletion layer, depletion zone, junction region, space charge region or space charge layer, is an insulating region within a conductive, doped semiconductor material where the mobile charge carriers have been diffused away, or have been forced away by an electric field. The only elements left in the depletion region are ionized donor or acceptor impurities. The depletion region is so named because it is formed from a conducting region by removal of all free charge carriers, leaving none to carry a current. In the depletion region of a semiconductor, the free carrier concentration is very small as compared to the bulk [44].

The width of the total depletion layer is $b_1$between the surface and the neutral region is given by the sum of the width of the highly depleted layer (b_s) and the width of the transition region (b_δ) between the highly depleted region and the quasi-neutral region:

$$b_1 = b_s + b_\delta \,. \tag{2-13}$$

The band bending in different layers accounts for the variation of the majority carrier concentrations in these layers. The description of the band bending, $E(x)$ at any location x in the depletion region also enables us to evaluate the thermal equilibrium free carriers densities at any point x in the depletion region. The majority carrier density, $p(E)$ at any energy, E in the depletion layer of a p-type semiconductor can be expressed as [45, 46]:

$$p(E) = p_0 \exp\left(-\frac{E}{k_B T}\right). \tag{2-14}$$

The majority carrier concentration in Eqn. (2-14) is in general decreases with increasing the band bending. The minority carrier concentration at any point in the depletion layer can be described using the law of mass action, Eqn. (2-9) and along with Eqn. (2-14) as:

$$n(E) = n_0 \exp\left(\frac{E}{k_B T}\right). \tag{2-15}$$

The position dependence of the bending in energy at depth x below the surface is given by:

$$E(x) = -\frac{e^2 N_a^-}{2\varepsilon}(b_1 - x)^2. \tag{2-16}$$

Where $E(x)$ is the band bending at depth x, N_a^- is doping concentration, k_∞ is dielectric constant (14.4) and ϵ_0 is permittivity of free space $\left(8.85 \times 10^{-12}\,\frac{c^2}{Jm}\right)$. b_1 is width of the total depletion region for p-type material [47].

$$b_1 = \sqrt{\frac{2\varepsilon E_s}{e^2 N_a^-}}. \tag{2-17}$$

The thermal equilibrium majority carrier density at the surface ($x = 0$) of a p-type semiconductor can also be expressed in terms of the surface Fermi-level position, E_{SF} The majority carrier at the surface ($x = 0$) for p-type semiconductor is hence given by:

$$p_{0S} = p_0 \exp\left(\frac{-E_S}{k_B T}\right). \tag{2-18}$$

Where E_S the energy bending at the surface ($x = 0$) described as:

$$E_S = -\frac{e^2 N_a^-}{2\varepsilon} b_1^2. \tag{2-19}$$

$$E_{SF} = E_{BF} + E_S. \tag{2-20}$$

Where the Fermi-level position, E_{BF} relative to the VBM in the bulk for p-type semiconductor is given by [17]:

$$E_{BF} = E_i - k_B T ln\left(\frac{p_0}{n_i}\right). \tag{2-21}$$

2.4 Statistics of donors and acceptors

The density of electrons in a shallow-donor state is given by:

$$n_d = \frac{N_d}{1 + \frac{1}{g_d}\exp\left(\frac{E_d - E_F}{k_B T}\right)}, \tag{2-22}$$

where, n_d is the density of electrons occupying the donor level is, N_d is the concentration of donor atoms, E_d is the energy of the donor level and g_d is the donor-site degeneracy factor.

The concentration of ionized donors N_d^+ is then:

$$N_d^+ = N_d - n_d = \frac{N_d}{1 + \frac{1}{g_d}\exp\left(\frac{E_F - E_d}{k_B T}\right)}. \tag{2-23}$$

When a singly ion sable donor captures an electron it becomes neutral, and when it releases an electron, it becomes positively charged. Using the same analysis, the concentration of ionized acceptors N_a^- we have:

$$N_a^- = N_a - p_a = \frac{N_a}{1 + g_a \exp\left(\frac{E_F - E_a}{k_B T}\right)}, \tag{2-24}$$

where, p_a is the density of holes bound to acceptors, N_a the concentration of acceptor atoms, E_a the energy of the acceptor level relative to the valence band, N_a^- the concentration of ionized acceptor atoms and g_d is the acceptor-site degeneracy factor. When a singly ion sable acceptor captures an electron it becomes negatively charged, and neutral when it releases the electron. When free electron-hole pairs annihilate through recombination, the free carrier concentrations in the conduction

and valence bands adjust for the intrinsic semiconductor $n_0 = p_0 = n_i$ For the extrinsic semiconductors this takes the form:

$$n_0 = N_d^+ + \mathfrak{N} - n_R \qquad \text{and} \qquad p_0 = N_a^- + \mathfrak{N} - n_R, \tag{2-25}$$

where n_R is the concentration of the total electron-hole pairs being annihilated each other after the donors and the acceptors are being ionized, $\mathfrak{N}$ is the concentration of electron-hole pairs thermally generated from band to band, N_d^+ and N_a^- are the densities of free electrons and holes contributed by the donor and the acceptor levels to the respective conduction and valence bands. Upon eliminating $\mathfrak{N} - n_R$ in Eqn. (2-25) the well-known neutrality relationship is obtained:

$$\mathrm{n}_0 + N_a^- = p_0 + N_d^+. \tag{2-26}$$

The law of mass action Eqn. (2-9) along with Eqns. (2-23) and (2-24) yields:

$$p_0 = \frac{N_a^- - N_d^+}{2} \sqrt{n_i^2 + \left(\frac{N_a^- - N_d^+}{2}\right)^2}. \tag{2-27}$$

For very high acceptor impurity concentrations $(N_a^- >> N_d^+)$ Eqn. (2-27) can be simplified:

$$p_0 = N_a^- + n_i. \tag{2-28}$$

2.5 Photon absorption in semiconductors

Next, we are going to investigate a photon absorption rate at the surface and in the bulk of a very thick semiconductor. A semiconductor can absorb a photons having $h\nu > E_g$. This energy can be supplied in the form of light. Each light photon has energy:

$$E_{ph} = h\nu. \tag{2-29}$$

where h is the Planck's constant and ν is the frequency of the light. Photons incident on the surface of a semiconductor are reflected, transmitted and absorbed (or scattered) components. The absorbed photon has the possibility of exciting an electron from the valence band to the conduction band. The photo-response of the material can be measured through the change in the photoconductivity due to the absorbed photons. The term "photo-conductivity" refers to a change in conductivity of a semiconductor when illuminated by photons. The generation of excess electron-hole pairs in a semiconductor is known as the injection of excess carriers [48]. At thermal equilibrium, the valence band contains many electrons and the conduction band has many empty states into which electrons may be excited. When photons with energies equal to or

greater than the band gap are incident on semiconductor materials, the photons are absorbed by the formation of electron-hole pairs. While the photo-generated carriers exist in their respective bands, they are free to contribute to the conductivity of the material. The electron-hole pairs generated by photon absorption are known as photo-generated carriers. In the case of a pure semiconductor, photons with energy less than the band gap energy will not be enough to excite an electron from the valence band to the conduction band and it will pass through the semiconductor without being absorbed [28].

2.5.1 Absorption in infinitely thick semiconductors

Thick (bulk) semiconductor can be described when the thickness of the semiconductor,b is infinitely large($b \to \infty$). Figure 2-4 shows a photon beam of flux density $\Phi_0(cm^{-2}s^{-1})$ directed at the upper surface of a portion of a semiconductor sample of length l, width w and infinitely large thickness. It is assumed that the beam contains only photons of energy $\hbar\omega \geq E_g$ selected by a monochromator [49].

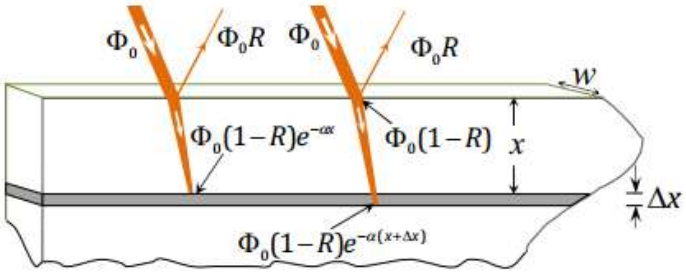

Figure 2-4: Absorption of photons in an infinitely thick (bulk) semiconductor [8].

The photon absorption rate (g_0) in entire volume of the given illuminated area (A) and thickness (Δx) is defined as the total number of absorbed photons per unit volume per unit time:

$$g_0 = \frac{\Delta N_{ph}}{A\Delta x\Delta t} = \frac{\Delta\Phi}{\Delta x}, \tag{2-30}$$

where ΔN_{ph} is the number of absorbed photons, Δt the time and ΔΦ the absorbed photon flux density is given as:

$$\Delta\Phi = \frac{\Delta N_{ph}}{A\Delta t}, \tag{2-31}$$

As the beam passes through the sample, the photon flux density at a distance x from the surface can be calculated by considering the probability of absorption within any infinitesimal thickness dx. The photon absorption rate at depth x for a given wavelength is also proportional to the photon flux density, $\Phi(x)$ remaining at x after being absorbed in the preceding section of material [50]:

$$G_0 = \frac{d\Phi(x)}{dx} = -\alpha\Phi(x)\,, \tag{2-32}$$

Where α is a constant called the absorption coefficient, which is related to the dielectric properties of the material and the wavelength of the incident photons. The negative $(-)$ sign in Eqn. (2-32) indicates the decrease g_0 with increasing x. The value of the absorption coefficient is determined using its dependence on the photon energy, analyzed by Bardeen et al [51, 16, 7].

$$\alpha(\omega) = \frac{2^{\frac{2}{3}} m_n e^2}{3\hbar^2\sqrt{k_\infty}} \left(\frac{m_n^* m_p^*}{m_n\left(m_n^* + m_p^*\right)}\right)^{\frac{3}{2}} \left(1 + \frac{m_n}{m_n^*} + \frac{m_n}{m_p^*}\right) \left(\frac{\hbar\omega - E_g}{m_n c^2}\right)^{\frac{1}{2}}. \tag{2-33}$$

Here, $\hbar = \frac{h}{2}$ is the reduced Plank's constant, e is the elementary charge, m_n is the free electron mass, c the speed of light and $m_{n/p}^*$ is the effective electron/hole mass. This allows

$\alpha(v)$ to be calculated for all wavelengths of the incident photons. Taking into account the reflection of a photon flux density $\Phi_0 R$ back to the vacuum or air, the photon flux density entering the illuminated surface is given by the difference between the incident and the reflected photon flux densities:

$$\Phi_s(0) = \Phi_0(1 - R), \tag{2-34}$$

The photon flux density at distance *x* below the illuminated surface, using the boundary condition in Eqn. (2-34), results in:

$$\Phi(x) = \Phi_0(1 - R)e^{-\alpha x}. \tag{2-35}$$

Eqn. (2-35) is known as Beer's law [45]. The reflection coefficient (reflectivity) R is calculated assuming that the refractive index, n remains constant for the entire wavelength range under consideration, i.e. $\lambda < 20\mu m$. For $GaSb$, the refractive index was taken as 3.8. This results in a typical value of $R \approx 0.34$ [52, 53].

The photon flux density absorbed in the elemental thickness δx at a distance x below the illuminated surface can be described from Eqns. (2-32) and (2-35) as:

$$\delta\Phi = \alpha\Phi_0(1-R)e^{-\alpha x}\delta x. \tag{2-36}$$

Equations (2-30) and (2-36) yield the photon absorption rate for different wavelengths as:

$$g_0(\alpha, \mathrm{x}) = \alpha\Phi_0(1-R)e^{-\alpha x}. \tag{2-37}$$

The photon absorption rate in Eqn. (2-37) also depends on the absorption coefficient α. The linear term dominates for lower values of α , while the exponential term dominates for higher values of α .It has a maximum value for intermediate values of α,which can be found by differentiating Eqn. (2-37) with respect to α and equating it to 0:

$$\frac{dg_0(\alpha, x)}{d\alpha} = 0. \tag{2-38}$$

The depth x at which $g_0(\alpha, x)$ has a maximum value for a given photon energy is called the penetration depth $(x_p)$of that photon:

$$x_p = \frac{1}{\alpha}. \tag{2-39}$$

Taking into account (*2-39*) along with Eqn. (*2-37*) gives:

$$g_0(x_p, \mathrm{x}) = \frac{\Phi_0(1-R)}{x_p} exp\left(\frac{-x}{x_p}\right). \tag{2-40}$$

The maximum value of the absorption rate at the penetration depth, x_p for a photon with particular absorption coefficient, α can be determined using Eqns.(2-40) and (2-39) as:

$$g_0(x_p) = \frac{\Phi_0(1-R)}{x_p} exp(-1) = 0.37\left(\frac{\Phi_0(1-R)}{x_p}\right). \tag{2-41}$$

The photon absorption rate in Eqn. (2-40) has maximum value at the surface when $(x \to 0)$ given as:

$$g_0(x_p) = \frac{\Phi_0(1-R)}{x_p}. \tag{2-42}$$

The limiting cases for the photon absorption rate in a very thick semiconductor can be concluded as:

$$g_0 = \begin{cases} \Phi_0\alpha(1-R), & \text{for } x < \dfrac{1}{\alpha} = x_p \ , \\ \dfrac{\alpha\Phi_0(1-\mathrm{R})}{\mathrm{e}}, & \text{for } x = \dfrac{1}{\alpha} = x_p \ , \\ 0, & \text{for } x > \dfrac{1}{\alpha} = x_p . \end{cases} \tag{2-43}$$

The absorption rate falls to 37% of the maximum value at the surface or takes the form of Eqn. (2-41) at the absorption depth (x_p), and goes to zero when the values of x is much exceeding the values of the absorption depth (x_p) of the absorbed photon or $(x \to \infty)$.

2.5.2 Absorption in a thin semiconductor film

Semiconductor thin films are ranging from fractions of a nanometre to several micrometres in their thicknesses (b), multiple reflections and transmissions of photons can occur at both the top and the bottom surfaces when they are illuminated. Very thin semiconductor films are mainly dominated by the under surface depletion layers, so that their photo-response is surface influenced than the bulk. The absorption rate will depend on the thickness of the sample and the reflection from both surfaces for a thin film. Figure 2-5 depicts a double-sided sample of thickness b, illuminated by a source with photon flux density Φ_0. Each time the radiation meets a surface, some photons are reflected and some are transmitted. The processes of reflection, transmission and absorption are repeated many times until all the photons are absorbed by the material and transmitted through the surfaces. The expressions and the arrows in the Figure 2-5 describes the incident, reflected and transmitted rays at the boundaries (top and bottom surfaces) of the sample.

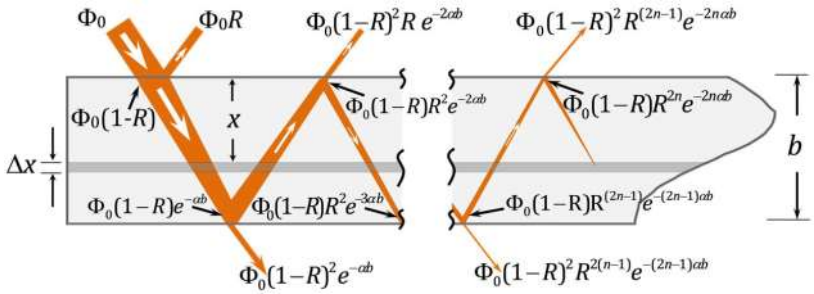

Figure 2-5: Absorption of photons in a semiconductor film [8].

The photon flux density transmitted through the bottom surface after n^{th} order is given by:

$$\Phi_{BT,n} = \Phi_0(1-R)^2 R^{2(n-1)} \exp[-(2n-1)\alpha b]\,, \quad (n = 1,2,3\ldots). \tag{2-44}$$

The photon flux density reflected back to the sample from the bottom surface after n^{th} order is given by:

$$\Phi_{BR,n} = \Phi_0(1-R)^2 R^{(2n-1)} \exp[-(2n-1)\alpha b]\,, \quad (n = 1,2,3\ldots). \tag{2-45}$$

The photon flux density transmitted through the upper surface after n^{th} order is given by:

$$\Phi_{UT,n} = \Phi_0(1-R)^2 R^{(2n-1)} \exp[-2n\alpha b]\ , \quad (n = 1,2,3\ldots). \tag{2-46}$$

The photon flux density reflected back to the sample from the upper surface after n^{th} order is given by:

$$\Phi_{UR,n} = \Phi_0(1-R) R^{2n} \exp[-2n\alpha b]\ , \quad (n = 1,2,3\ldots). \tag{2-47}$$

The total photon flux density absorbed in the sample, $\Delta\Phi$ is then given by the difference between the incident photon flux density, Φ_0 and the total flux density leaving the sample, $\Phi_R + \Phi_T$:

$$\Delta\Phi = \Phi_0 - (\Phi_R + \Phi_T) = \frac{\Phi_0(1-R)(1-exp^{-\alpha b})}{1-Rexp^{-\alpha b}} \tag{2-48}$$

The photon flux density entering a thin section with thickness Δx at depth x as positive and that leaving the section as negative, one can show that the photon flux density at the top surface of the section Δx of the material shown in Figure 2-5 is:

$$\Phi(x) = \frac{\Phi_0(1-R)\mathrm{e}^{-\alpha x}}{1-R^2\mathrm{e}^{-2\alpha b}}[1 - Rexp - 2\alpha(b-x)] \tag{2-49}$$

The photon flux density absorbed in Δx is then given by the difference in the photon flux density on either side of this section:

$$\Delta\Phi = \frac{\Phi_0(1-R)\mathrm{e}^{-\alpha x}(1-\mathrm{e}^{-\alpha\Delta x})}{1-R^2\mathrm{e}^{-2\alpha b}}\left[1 + R\mathrm{e}^{-\alpha[2(b-x)-\Delta x]}\right]. \tag{2-50}$$

The photon absorption rate in this layer of thickness Δx is:

$$g_0(\alpha, x, \Delta x) = \frac{\Phi_0(1-R)\mathrm{e}^{-\alpha x}(1-\mathrm{e}^{-\alpha\Delta x})}{(1-R^2\mathrm{e}^{-2\alpha b})\Delta x}\left[1 + R\mathrm{e}^{-\alpha[2(b-x)-\Delta x]}\right]. \tag{2-51}$$

For very small Δx we can assume $2(b-x) - \Delta x \approx 2(b-x)$ and $1 - e^{-\alpha\Delta x} \approx \alpha\Delta x$, so that the photon absorption rate at a distance x below the illuminated surface of the sample can be written as:

$$g_0(\alpha, x) = \frac{\alpha\Phi_0(1-R)\mathrm{e}^{-\alpha x}}{1-R^2\mathrm{e}^{-2\alpha b}}\left[1+R\mathrm{e}^{-2\alpha(b-x)}\right]. \tag{2-52}$$

At the top (illuminated) surface, $x = 0$ so that:

$$g_0(\alpha, 0) = \frac{\alpha\Phi_0(1-R)}{1-R^2\mathrm{e}^{-2\alpha b}}[1+R\mathrm{e}^{-2\alpha b}]. \tag{2-53}$$

and at the bottom surface, $x = b$, so that:

$$g_0(\alpha, x) = \frac{\alpha\Phi_0(1-R^2)\mathrm{e}^{-\alpha b}}{1-R^2\mathrm{e}^{-2\alpha b}} \tag{2-54}$$

The total photon absorption rate in the entire sample of thickness b can be determined from Eqn. (2-51) by changing Δx to the sample thickness b and taking the depth to the surface ($x \to 0$)as:

$$G_0(\alpha, b) = \frac{\Phi_0(1-R)(1-\mathrm{e}^{-\alpha b})}{b(1-R\mathrm{e}^{-2\alpha b})}, \tag{2-55}$$

The limiting values of the total photon absorption rate in a given sample can be generalized from Eqn. (2-55) as:

$$G_0(\alpha, b) = \begin{cases} \alpha\Phi_0, & \text{for } \alpha < \dfrac{1}{b}, \\ \dfrac{\Phi_0(1-R)(e-1)}{b(e-R)}, & \text{for } \alpha = \dfrac{1}{b}, \\ \dfrac{\Phi_0(1-R)}{b}, & \text{for } \alpha > \dfrac{1}{b}. \end{cases} \tag{2-56}$$

2.6 Optical generation and recombination of excess carriers

2.6.1 Generation/recombination rate equation

The rates of change of electrons in the conduction band and holes in the valence band are equal and always given by the difference between the generation and the recombination rates [8], i.e.:

$$\frac{dn}{dt} = \frac{dp}{dt} = G - R, \tag{2-57}$$

Where n and p represent the non-thermal equilibrium electron and hole concentrations in the conduction and valence bands respectively, and G and R are the total generation and recombination rates of charge carriers, respectively. The total generation rate involves both the thermal (G_{th}) and optical (G_0) generation rates:

$$G = G_{th} + G_0, \tag{2-58}$$

The net excess carrier recombination rate U is defined as the difference between the total recombination rate and the thermal equilibrium generation rate:

$$U = R - G_{th}, \tag{2-59}$$

The net recombination rates for photo-generated electrons and holes are given by:

$$U = \frac{\delta_n}{\tau_n} = \frac{\delta_p}{\tau_p}, \tag{2-60}$$

where δ_n and δ_p are the concentrations of photo-generated carriers.

The parameters τ_n and τ_p are called the electron and hole recombination lifetimes, respectively. Using thermal equilibrium conditions and the principle of detailed balance along with Eqns. (2-57) to (2-60), the rates of change of the excess carriers are:

$$\frac{d\delta_n}{dt} = G_0 - U = \frac{d\delta_p}{dt}. \tag{2-61}$$

Electron-hole pairs are continuously generated under illumination, and the excess charge carrier concentrations will increase. Recombination, on the other hand, tries to reduce the excess carrier concentrations to zero.

2.6.2 Recombination mechanism in semiconductors

In a semiconductor material, recombination mechanisms can in general be classified into two groups, radiative and non-radiative [54]. Radiative recombination is the radiative transition of an electron in the conduction band to an empty state (hole) in the valence band. The optical processes associated with radiative transitions are (i) spontaneous emission, (ii) absorption, and (iii) stimulated emission. Stimulated emission, in which the emitted photon has exactly the same energy and momentum as the incident photon, forms the basis for laser action. Non-radiative recombination of an electron-hole pair as the name implies, is characterized by the absence of a photon emission in the recombination process. The parameters like temperature, carrier concentration and carrier life time have significant effect on non-radiative recombination [9]. Non-radiative recombination occurs when excess energy is released as phonons or transferred as excess kinetic energy to another charge carriers. Hence, the excess energy is dissipated as heat during the recombination process [55].

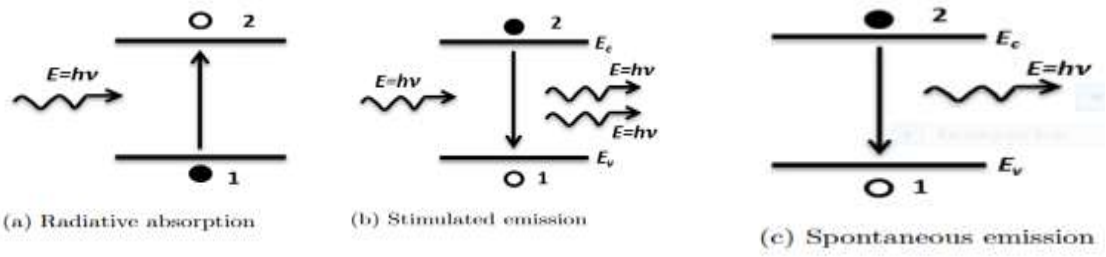

Figure 2-6: Band-to-band radiative transitions

2.6.2.1 Radiative recombination

Radiative recombination is the fundamental microscopic quantum process that leads to light emission in semiconductors and the operation of LEDs. It occurs vertically in the band-structure diagram and enables photon emission in light-emitting diodes. The radiative recombination is the inverse process of fundamental optical absorption in a semiconductor. The recombination of an electron and holes take place with the release of energy which is equal to the initial difference in the energies of the two charged particles. The released energy is given out in the form of radiation. Radiative recombination is the frequency of the radiation falls within the visible range, a photon is said to be emitted. Radiative recombination is a direct recombination mechanism, in which the electrons in the conduction band decay to the valence band (i.e. recombine with holes in the valence band) [56]. This is a very efficient process in direct band gap semiconductors. The energy lost by an electron in making the transition is released as a photon. The total recombination rate (R) is directly proportional to the product of the concentration of electrons n available in the conduction band and the concentration of holes p available in the valence band [57].

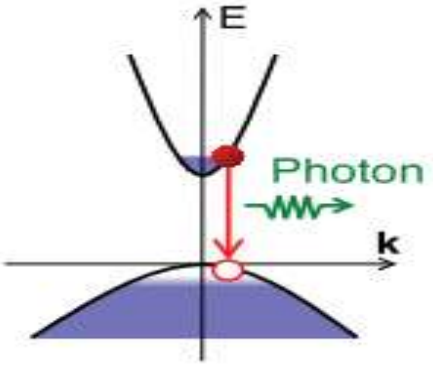

Figure 2-7: radiative recombination [42].

$$R = C_R np, \tag{2-62}$$

Where C_R is a constant known as the coefficient of holes in the valence band for the capture of electrons, and is related to the electron capture cross-section (σ_R) and the thermal velocity of the electrons (ϑ_{th}):

$$C_R = \sigma_R \vartheta_{th}. \tag{2-63}$$

The band-to-band capture coefficient for bands with spherical symmetry was shown by van Roosbroeck and Shockley to depend on the absorption coefficient through the relation [58]:

$$C_R = \frac{8\pi k_\infty}{c^2} \int_0^\infty \frac{\alpha(\upsilon)\upsilon^2 d\upsilon}{exp\left(\frac{h\upsilon}{k_B T}\right) - 1} \quad , \tag{2-64}$$

Where $\alpha(\upsilon)$ the absorption coefficient, h is Planck's constant and c is the speed of light. Values of C_R can be obtained by numerical integration of Eqn. (2-64) for narrow band gap semiconductors as [58, 59]:

$$C_R = e\pi\sqrt{k_\infty}\left(\frac{m_n}{m_n^* + m_p^*}\frac{300}{T}\right)^{\frac{3}{2}}\left(1 + \frac{m_n}{m_n^*} + \frac{m_n}{m_p^*}\right)\left[E_g^2 + 3E_g k_B T + 3.75 k_B^2 T^2\right], \tag{2-65}$$

where E_g and $k_B T$ are in electron volt (eV).

For large band gap materials where $E_g \gg k_B T$ only the E_g^2 term is needed. Figure 2-8 shows the radiative recombination coefficient as function of temperature. As we observed from the Figure 2-8 the radiative coefficient decreases with temperature increases and increases as the temperature decreases. Since, $E_g \gg k_B T$ the term E_g^2 is dominant in this case as predicted [22].

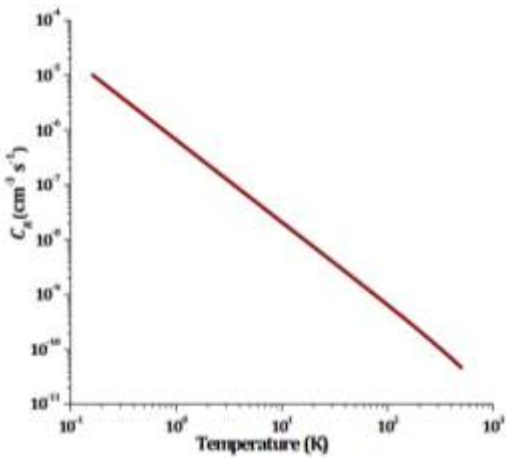

Figure 2-8: Radiative recombination coefficient as function of temperature for GaSb.

There are two principal categories of carrier lifetimes: Recombination lifetimes and generation lifetimes. The concept of recombination lifetime τ_R holds when excess carriers decay as a result of recombination. The generation lifetime τ_g by analogy, is the time that it takes on average to generate an ehps. The net photo-generated carrier recombination rate in the absence of excess carrier traps is given by the difference between the non-thermal equilibrium recombination rates, Eqn. (2-62) and the thermal equilibrium recombination rate:

$$R_0 = C_R n_0 p_0 = C_R n_i^2 = R_{th} \quad , \tag{2-66}$$

But, in non-equilibrium electron-hole densities, $np > n_i^2$ and $\delta n = n - n_{o,}\ \delta p = p - p_o$. in a non-degenerate semiconductor, the rate at which electrons and holes are annihilated via band-to-band Radiative recombination is proportional to the product of electron and hole densities in the conduction and valence bands. The net carrier recombination rate *(U_{Rad})*, is obtained by solving Eqns. (2-62) and (2-66) resulting in:

$$U_R = R - R_{th} = C_R(np - n_i^2) \tag{2-67}$$

Inserting non-equilibrium concentration $n = n_o + \delta n$ and $p = \delta p + p_o$ into equation (2-67) and for the case of low-level injection, the excess carrier concentration δn and δp with $\delta n = \delta p$, then the following general expression for radiative recombination rate, U_R is given by:

$$U_R = C_R \delta n(\delta n + p_0 + n_0) \tag{2-68}$$

The excess carrier lifetimes under steady-state conditions are defined by the ratio of the excess carrier density and the net capture rate for electrons and holes, and are given respectively by [60]:

$$\tau_n = \frac{\delta n}{U_R}, \quad \text{for electrons} \tag{2-69}$$

$$\tau_p = \frac{\delta p}{U_R}, \quad \text{for holes} \tag{2-70}$$

So, the radiative excess carrier lifetime, τ_R takes the form [61, 15, 62]:

$$\tau_R = \frac{\delta n}{U_R} = \frac{1}{C_R(n_0 + p_0 + \delta n)} \tag{2-71}$$

From Eqn. (2-71), it is noted that the radiative lifetime τ_R is inversely proportional to the carrier density because in band-to-band recombination both electrons and holes must be present simultaneously. The injection level is important during lifetime measurements. Low-level injection holds when the excess minority carrier density is low compared to the equilibrium majority carrier density, ($\delta n \ll p_0 + n_0$), similarly, high level injection holds when ($\delta n \gg p_0 + n_0$). Eqn. (2-71), simplify for both low-level and high-level injection [63].

For a material under low injection level ($\delta n \ll p_0 + n_0$), Eqn. (2-71) can be simplified to:

$$\tau_R = \tau_{R0} = \frac{1}{C_R(n_0 + p_0)}, \tag{2-72}$$

For a material under high injection level ($\delta n \gg p_0 + n_0$), then:

$$\tau_R = \frac{1}{C_R \delta n}, \tag{2-73}$$

Using Eqns. (2-72), (2-67) and (2-61), one can determine the rate of excess free carrier accumulation:

$$\frac{d\delta_n}{dt} = G_0 - \left(\frac{\delta_n}{\tau_{R0}} + C_R \delta n^2\right). \tag{2-74}$$

Using the initial condition $\delta_n \approx 0$ at time =0, the steady-state solution to Eqn.(2-74) becomes:

$$\delta n(t) = \frac{2G_0 \tau_k \tau_{R0}}{\tau_{R0} + \tau_k}, \tag{2-75}$$

where τ_k is the time constant given by:-

$$\tau_k = \frac{\tau_{R0}}{\sqrt{1 + 4C_R G_0 \tau_{R0}^2}}, \tag{2-76}$$

The radiative recombination and generation lifetimes are then given by:

$$\tau_R = \tau_g = \frac{2\tau_k \tau_{R0}}{\tau_{R0} + \tau_k}. \tag{2-77}$$

The excess carrier lifetime is in general determined by the recombination rate of the minority charge carriers at the surface and in the bulk of the material. For a steady state condition, the excess carrier generation rate (G_0) is equal to their reverse recombination rate (R).

Chapter 3 : Methodology

This chapter gives the details explanation through which the calculations are done and the method that used. The majority carrier concentration, p_0 and surface fermi level position, (E_{SF}) used in the analysis for different doping levels GaSb samples were taken from the simulation of the existing temperature dependence Hall measurements data measured at Nelson Mandela Metropolitan University, South Africa. The minority carrier concentration, n_0 is determined from p_0 and the intrinsic carrier concentration using the law of mass action for a particular semiconductor using the relation in Eqn.(2-15). The energy bending at the surface, E_S is determined from E_{SF} and the Fermi-level position relative to the VBM in the bulk for highly doped p-type semiconductor by the relation (2-20).

Then, the photon absorption rate in the bulk semiconductor is described using the technique discussed in Section 2.5.1. The model of bulk semiconductor was illustrated in Figure 2-4. By using illumination mechanisms, the photon absorption rate at the surface and in the bulk of semiconductors were studied in details and the variation of the photon absorption rate with the depth x below the illuminated surface at different temperatures in bulk semiconductor were determined from the relation in Eqn. (2-37). In the thin film semiconductor was also modelled to determine photon absorption effect in different layers of thin film semiconductors as illustrated in Figure 2-5. Also, by using illumination mechanisms, the total photon flux density and photon absorption rate in a layer of thickness Δx situated at depth x below the illuminated surface were investigated in details. By taking a sample of thin film of thickness b with depletion layers of equal thicknesses b_1 on either sides under the two surfaces, the photon absorption rate effect in each layer of a thin film semiconductor are also determined. Moreover, the photon absorption rate at a point situated x distance below the illuminated surface and the total photon absorption rate in the entire sample of thickness b were described using Eqns. (2-52) and (2-55), respectively. In the analysis of this result, the vertical axis for the photon absorption rate and horizontal axis for the depth below the illuminated surface was taken as semi-log for both thin film and bulk semiconductors. Then, the temperature dependence of the low injection level thermal equilibrium carrier concentrations and band bending energy of the thin film Gallium

Antimonide (GaSb) was investigated by considering the variation of the energy bending at the surface.

Finally, by using the steady-state radiative recombination mechanism for small band gap of semiconductor, the expression for the radiative excess carrier lifetime as function of depth below the illuminated surface of the GaSb material was obtained in terms of the temperatures, the injection levels and absorption coefficients. The results of the analyses were described using semi-log graphs for all the excess carrier lifetimes. The effects of the temperatures, the energy and the injection level of the illuminations on the photo-response of the under surface depletion layer and the deep bulk of given semiconductor for single doping are discussed in detail in the next chapter.

Chapter 4 : Results and discussion

This chapter deals with the analysis and discussion of the entire results of this work. First, the photon absorption rate in both the bulk and thin films semiconductors were determined and compared. Then, Variations of the Energy bending and the thermal equilibrium carrier concentrations in the under surface depletion layer and the deep bulk of p-type semiconductor were continued. Finally, the photo-response (excess carrier lifetimes) for both bulk and thin films semiconductors were analyzed.

4.1 Photon absorption rate in both bulk and thin film semiconductor

4.1.1 As function of depths at different temperatures

The photon absorption rate in this case is obtained as a function of depth below the illuminated surface of the sample using (2-37) and (2-52) for the bulk and thin films, respectively. Figure 4-1 shows the photon absorption rate in both the bulk and thin films as a function of depth below the illuminated surface for different absorption coefficients vary with temperatures. The brown curve shows the effects of absorption rate as function of depths x below the illuminated in thick semiconductor that has maximum value $\Phi_0\alpha(1-R)$ just at the illuminated surface. The green curve shows the effects of absorption rate as function of depths x below the illuminated in thin film semiconductor that has maximum value $\Phi_0\alpha$ just at the illuminated surface. As can be seen from Figure 4-1 the values of the absorption rate for the bulk material diminishes with increasing the depth below the illuminated surface and the maximum absorption rate at the illuminated surface is $\Phi_0\alpha(1-R)$. The values of the absorption rate for the thin material at low temperatures are low and constant pass through a thin material and the maximum absorption rate at the illuminated surface is $\Phi_0\alpha$. Absorption rate also decreases to $0.37\ \Phi_0\alpha(1-R)$ at α is equal to the reciprocal of the penetration depth of this particular photon in the material. One can also see from the Figure 4-1, temperatures with higher absorption

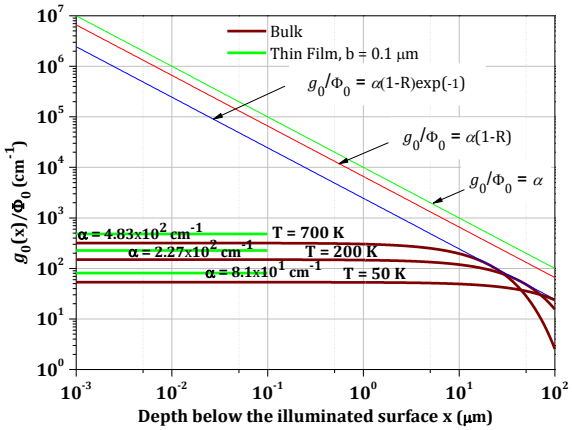

Figure 4-1: Comparison of photon absorption rate in both thin film and bulk semiconductor as a function of depth below the surface for different temperatures.

coefficients are absorbed more near the illuminated surface and temperatures with low absorption coefficients are passing through the materials without being absorbed.

Therefore, the difference between bulk and thin film semiconductors is that, in thick semiconductor, if a photon of flux density, Φ_0 is illuminating the surface, the amount $\Phi_0 R$ is reflected back and the absorption rate at depth x below the illuminated surface is given by Eqn. (2-37). Hence, the maximum absorption rate of $\Phi_0(1-R)$ occur just at the illuminated surface as shown by red lines in Figure 4-1. While, the absorption rate at depth x below the illuminated surface in thin film semiconductors which is described using relation in Eqn.(2-52) gives a maximum photon absorption rate $\Phi_0\alpha$ at the illuminated surface of thin film. This illustrates that, the reflection effect is compensated in thin films due to the multiple reflections of photon from the top and the bottom surfaces into the film. As a consequence, each point inside a thin film semiconductor has more photon absorption rates as compared to the corresponding points in thick semiconductors. The photon absorption rate in Figure 4-1 has in general three limiting values. These are, the maximum absorption rate just at the surface of a thin film represented by the green line, the maximum absorption rate just at the surface of a thick material represented by the red line and the absorption rate at the absorption depth under the illuminated surface of a thick material represented by the blue line. Therefore, one can conclude from this result shows that, the variation of the photon absorption rate in both thin and bulk of semiconductors with the depth below illuminated surface of the samples is increases with increasing temperatures.

4.1.2 As function of thickness of samples at different temperatures

The total photon absorption rate in both thin film and bulk semiconductor in this case is obtained as a function of thicknesses of the samples using Eqn.(2-55). The bulk semiconductor is a material with very large thickness and thin film corresponds to material with very small thickness$\left(b < \frac{1}{\alpha}\right)$. Figure 4-2 illustrates the total photon absorption rate in both thin film and bulk Semiconductor as function of thicknesses for different temperatures. As can be seen from Figure 4-2 the rate of absorption is increasing with decreasing thicknesses of the samples.

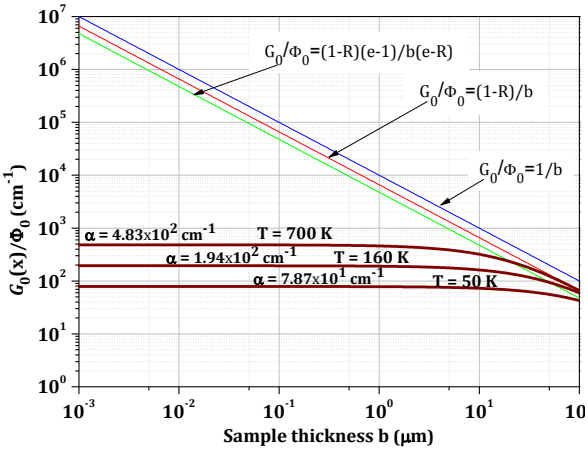

Figure 4-2: Total photon absorption rate in both thin film and bulk semiconductor as function of thickness for different temperatures

As can be seen from Figure 4-2 the rate of absorption is increasing with decreasing thicknesses of the samples. The variation of the absorption rate with the thicknesses of the samples is high for high temperatures and it is a constant rate for low temperatures in very thin films of different thicknesses, but is absorbed with different rates in thick films. Hence, the absorption rate increases with increasing the temperatures. The total photon absorption rate in Figure 4-2 has also three limiting values. These are, the maximum photon absorption rate in very thin film $\left(b < \frac{1}{\alpha}\right)$ represented by the blue line, the maximum photon absorption rate when the thickness of the material is equal to the penetration depth of the corresponding photon$\left(b = \frac{1}{\alpha}\right)$, represented by the green line and the photon absorption rate when the thickness of the material is greater than the penetration depth of the corresponding photon$\left(b > \frac{1}{\alpha}\right)$, represented by the red line. The variation of the photon absorption rates as function of the depths below illuminated surface is in good agreement with the results obtained by M. W. Shura photoconductive spectroscopy of GaSb films [8].

4.2 Position dependence of energy bending and thermal equilibrium carrier concentration of the thin film of Gallium Antimonide (GaSb)

4.2.1 Variation of energy bending with depth below the illuminated surface at different temperatures

Figure 4-3 illustrates the position dependence of doping level $2 \times 10^{17} cm^{-3}$ (a) energy band bending for samples with temperatures 60 K,150 K, 256 K, (b) energy band bending for samples with temperatures 256 K, 400 K, 500 K. The position dependence of the energy band bending in the under surface depletion layers and the bulk of thin film of Gallium Antimonide (GaSb) can be determined using Eqn.(2-16).

The width of the under surface depletion layers is also determined using relation (2-17).

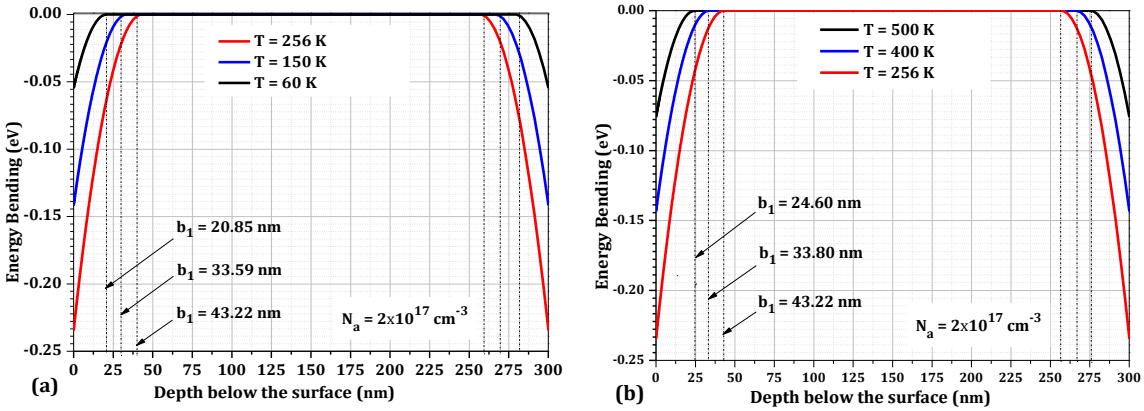

Figure 4-3: Position dependence of energy band bending in the thin film of Gallium Antimonide (GaSb) semiconductor.

Since the style of the variation of (a) the energy band bending with the depth below the illuminated surface for samples at different temperatures below 256 K is the same as that of (b) the variation of the energy band bending with the depth below the illuminated surface for samples at different temperatures above 256 K, except the difference in magnitude (size) as depicted in both Figure 4-3 (a) and (b). As can be seen from Figure 4-3 (a) and (b), the energy bending in the bulk region remains constant with depth below the illuminated surface, but in the entire depletion layer the energy bends down and reaches its maximum at the surface. As can be seen from Figure 4-3 (a) and (b), the temperatures above and below 256 K, hence the energy bending decreases at the two surfaces of a thin film semiconductor and the energy bending slightly decreases constant in the bulk region of a semiconductor. In addition, as seen from the figure that the width of the depletion region is maximum at 256 K and it is also in general decreases with increasing and decreasing temperatures. Therefore, one can conclude from this result also that, the band bending is decreasing at low temperatures than high temperatures at the two surfaces of a thin film semiconductor. This is an evidence that the temperature indicating a dominant surface conduction at low temperatures than high temperatures [64].

4.2.2 Variation of thermal equilibrium carrier concentrations with depth below the illuminated surface at different temperatures

The expression of the band bending energy, $E(x)$ at any location x in the depletion region also enables us to evaluate the thermal equilibrium free carriers concentrations at any point x in the depletion region already discussed in Figure 4-3 previously. The position dependence of the thermal equilibrium majority carrier concentration and minority carrier concentration in the under surface depletion layers and the bulk of thin film of Gallium Antimonide (GaSb) can be determined using Eqns. (2-14) and

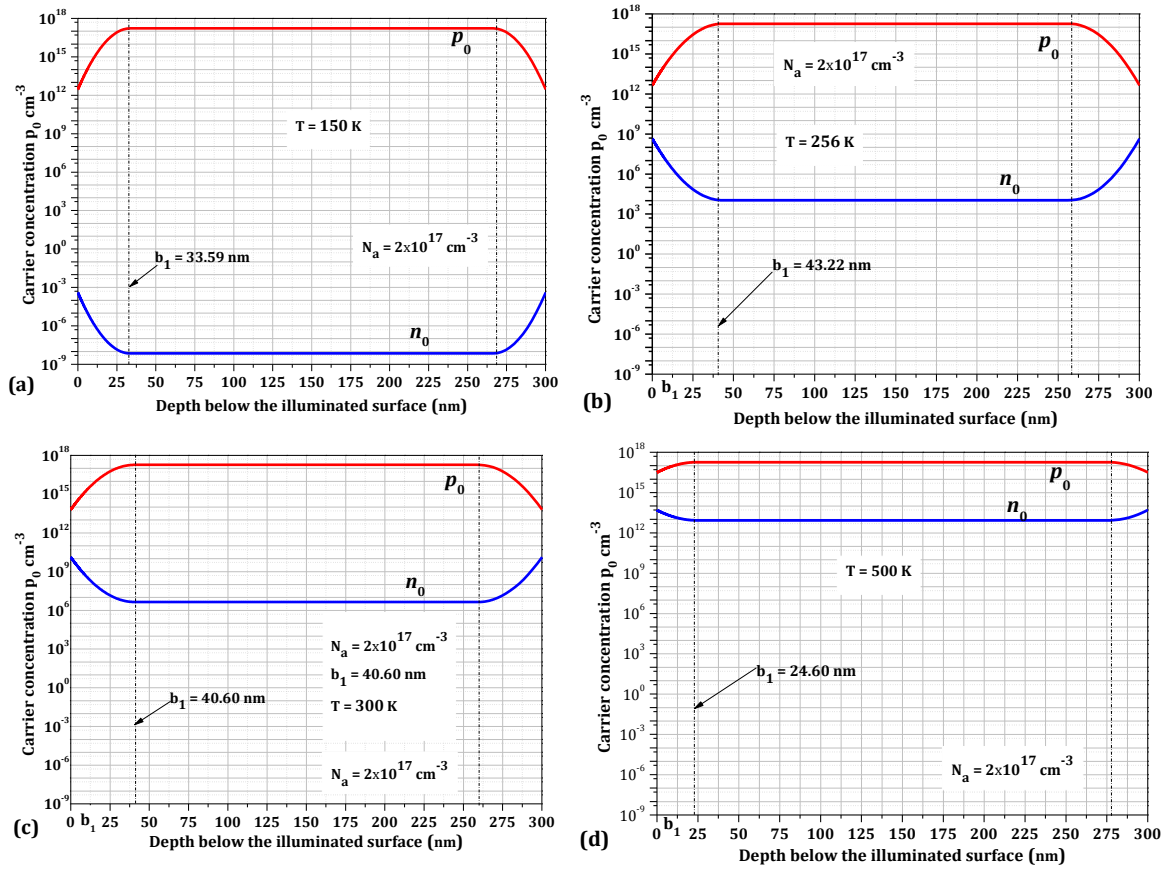

Figure 4-4: Position dependence of thermal equilibrium carrier concentration in the under surface depletion layer and the bulk of thin film of Gallium Antimonide (GaSb) semiconductor for different temperatures

(2-15), respectively. Figure 4-4 describes the position dependence of the thermal equilibrium carrier concentrations at different temperatures in the under surface depletion layer and the thin film of Gallium Antimonide (GaSb). From Figure 4-4 one can see that the majority carrier concentration in the depletion layer decreases from maximum value p_0 at the edge of the quasi-neutral region towards the surface and attains its minimum value in the entire region between the edge of the transition region and the surface, while the magnitude of the majority carrier concentration in the deep

bulk is fixed with depth below the illuminated surface. Since the band bending in different layers determines the variation of the majority carrier concentrations in these layers. The minority carrier concentration in the depletion layer increases from maximum value p_0 at the edge of the quasi-neutral region towards the surface and attains its maximum value in the entire region between the edge of the transition region and the surface and the magnitude of the minority carrier concentrations in the deep bulk is fixed with depth below the illuminated surface.

One can also see from Figure 4-4 the magnitude of the majority carrier concentration is constant in the deep bulk of the semiconductor with increasing the temperatures, while the magnitude of the majority carrier concentration is increasing under the both the surfaces of thin films of the semiconductor with increasing temperatures. The magnitude of the minority carrier concentration is highly increasing in both the deep bulk and the under surfaces of thin film of Gallium Antimonide (GaSb) with increasing the temperatures. This is an evidence that with the increasing temperatures both the majority and minority carrier concentrations become equal and approach the intrinsic concentration M. W. Shura photoconductive spectroscopy of GaSb films [8].

4.3 Determination of radiative excess carrier lifetime under different conditions

4.3.1 Low injection level and Low energy consideration

The photo-response of a semiconductor also depends on the temperatures. The radiative excess minority carrier lifetimes are determined by considering the variation of the majority carrier concentration with energy bending at different positions Eqn. (2-14) along with Eqn. (2-72). As already discussed in the previous section, the layer under the surface of Gallium Antimonide (GaSb) thin film is depleted of majority charge carriers and has very low thermal equilibrium majority carriers as compared to the deep bulk. This enhances the magnitude of the excess carrier lifetime in the under surface depletion layers than in the deep bulk. The low injection level radiative excess minority carrier lifetime is determined as a function of the depth below the illuminated surface for four samples with different temperatures 60 K,150 K, 256 K, 400 and

500 K by keeping the photon energy and the photon flux density at their possible lowest values.

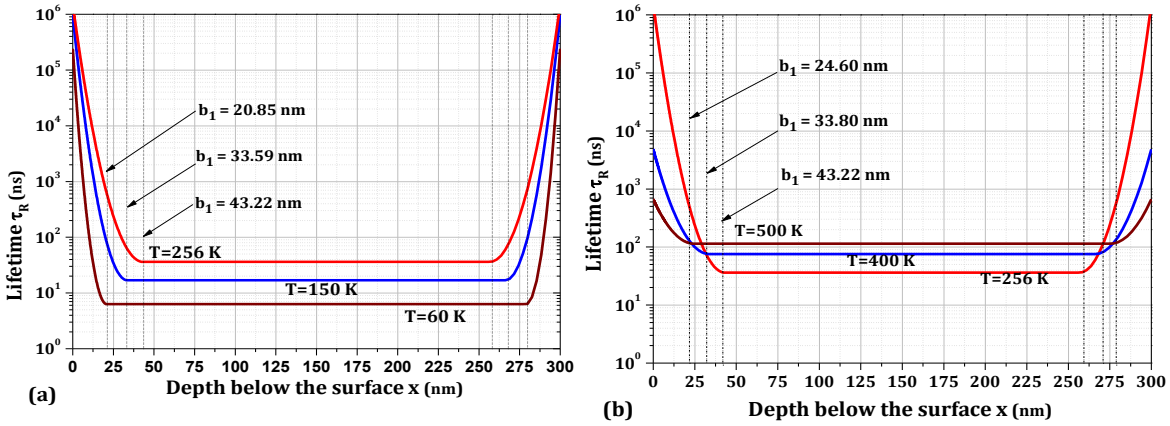

Figure 4-5 : Variation of radiative excess carrier lifetimes as function of the depth below surface for low injection level in thin film of GaSb sample and different temperatures.

The value of doping level and thickness for thin film GaSb used in this analysis is $2x10^{17}cm^{-3}$ and 300 nm, respectively. Figure 4-5 illustrates the variation of radiative excess carrier lifetime as function of the depth below the illuminated surface for low injection level in thin films of GaSb sample of thickness 300 nm with different temperatures, (a) below the 256 K temperatures, (b) above the 256 K temperatures.

Figure 4-5 (a) shows that; the magnitude of the radiative excess minority carrier lifetime is highly decreasing in the deep bulk of the semiconductor with decreasing the temperatures from the maximum of the depletion layer width for temperature 256 K, while the magnitude of the radiative excess minority carrier lifetime under the surface is slightly decreases with decreasing temperatures. Since majority carrier Concentration in the depletion layer decreases from maximum value p_0 at the edge of the quasi-neutral region towards the surface as discussed in Figure 4-4, attains its minimum value at the surface. Even though, the radiative excess minority carrier lifetime as shown in Figure 4-5 (b) is increasing and highly decreasing with increasing the temperatures from the maximum value of the depletion layer width for temperature 256 K for the deep bulk and under the surface of the semiconductor, respectively. Therefore, one can conclude from this result also that, the magnitude of the radiative excess minority carrier lifetime under the surface is insensitive to the below 256 K temperatures than above 256 K temperatures.

4.3.2 High injection level and absorption coefficients consideration

Figure 4-6 illustrates the depth below the illuminated surface dependence of doping level $2 \times 10^{17} cm^{-3}$ radiative excess minority carrier lifetimes for GaSb thin film with the photon flux density injection level is varied from 0 to $10^{32}\ cm^{-2}s^{-1}$ for, (a) Low absorption coefficient $10^{-3} cm^{-1}$, and (b) high absorption coefficient $10^{6}\ cm^{-1}$. At the surface regions have very low thermal equilibrium majority carrier concentration, p_{0S}, they always remain under high injection level condition under the situations where $p_{0S} < \delta n$, while the deep bulk with very high thermal equilibrium majority carrier concentration, $p_0 > \delta n$, still remains under low injection level as depicted by the two low injection levels 10^{24} cm^{-2}s^{-1} and 10^{27} cm^{-2}s^{-1} in Figure 4-6 (a). As can be seen from Figure 4-6 (a), the surface remains under high injection for all the illuminations except at 0 photon flux density, while the deep bulk is under high injection level only for the two high injection level illuminations with photon flux densities $10^{30} cm^{-2}s^{-1}$and $10^{32} cm^{-2}s^{-1}$. Since a photon with low energy can pass through a thin material with a constant low absorption rate as discussed in Figure 4-1, equal amounts of free carrier concentrations, δn are generated by the illuminations at all depths inside the material.

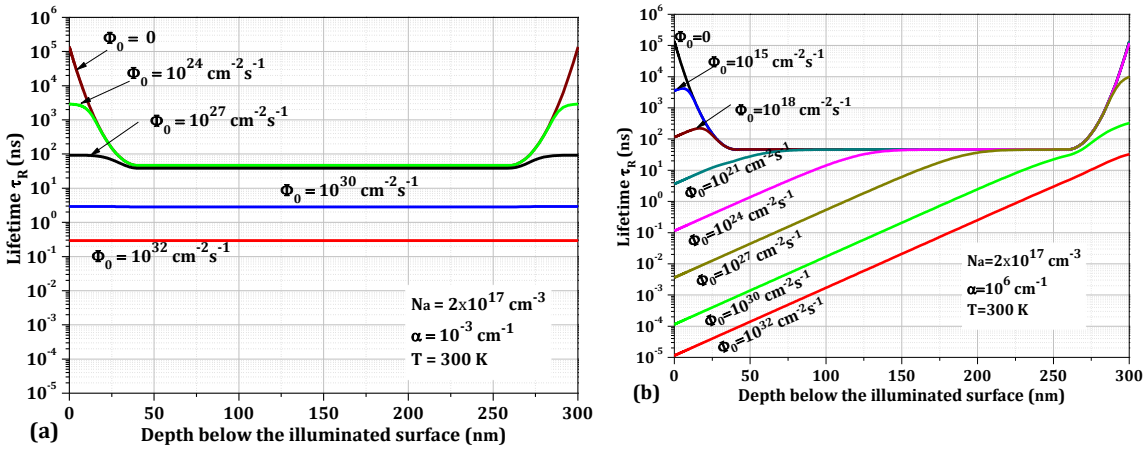

Figure 4-6: Variation of radiative excess carrier lifetimes as function of the depth below the illuminated surface for different injection level

Therefore, the photo response of the surface region is higher than the bulk in this case. With increasing the injection level of the photon flux density that can generate free carriers concentration more than the thermal equilibrium carrier concentrations in the bulk $p_0 < \delta n$ as indicated by the two higher injection levels $10^{30} cm^{-2}s^{-1}$ and $10^{32} cm^{-2}s^{-1}$, both the under surface layers and the deep bulk layers remain under the same high injection levels. As a consequence, the effects of high injection level and

low energy photons can be detected equally at all points inside a thin film material, while the effects of the low injection level and low energy photons cannot be detected in the deep bulk, but can be detected under the top and the bottom surfaces as illustrated in the Figure 4-6 (a). Therefore, one can conclude from this result also that, the excess carrier lifetime also decreases with increasing the injection levels for both the under surface layers and the bulk layer. The injection level dependence of the photo-response for p-type semiconductor material is in good agreement with the result obtained as that of M. Z. Rahman. [62].

As shown in Figure 4-6 (b), the absorption coefficient is kept at very high value $10^6 cm^{-1}$ and the fixed temp (300 K) as already seen in Figure 4-6 (a), the surface remains under high injection for all the illuminations except at 0 photon flux density, while the deep bulk is under low injection level only for the two low injection level illuminations with photon flux densities 10^{15} $cm^{-2}s^{-1}$ and 10^{18} $cm^{-2}s^{-1}$. The effects of these two injection levels cannot be detected in the deep bulk and under the bottom surface. Since the absorption rate of a photon with high energy is very high closer to the illuminated surface and decreases with increasing the depth below the illuminated surface as already discussed in detail in Figure 4-1, more amounts of free carrier concentrations, δn are generated by the illumination closer to the illuminated surface and this effect decreases with increasing the depth from the illuminated surface, so that the region under the bottom surface has minimum free carrier concentration.

The under surface regions still remain under high injection level condition for $p_{0S} < \delta n$, while the deep bulk with very high thermal equilibrium majority carrier concentration, p_0 shows different response at different positions to all the injection levels with the same higher photon energy. Due to the presence of maximum free carrier concentration under the illuminated surface, the excess carrier lifetime also has minimum value here as compared to the other points inside the material. The value of the excess carrier lifetime corresponding to each injection level also increases with increasing the depth below the illuminated surface and attains maximum value under the bottom surface where the free carrier's concentration is relatively very low. Hence, the effect of an illumination with high energy and high injection level can be detected at different points inside a material with various photo-responses. However, the effect of an illumination with high energy and low injection level can be detected only under

the illuminated surface as shown in Figure 4-6 (b). One can conclude from this result also that, the excess carrier lifetime also decreases with increasing the injection levels. In general, the effect of very high energy illumination is detected only under the illuminated surface, as a result of the absorption rate of a photon with high energy is very high closer to the illuminated surface. The variation of the photo-response of p-type GaSb films as function of the injection levels are in complete agreement with the results obtained by M. W. Shura *et.al* by steady state photoconductivity measurements [22, 17].

Chapter 5 : Conclusion

In this study, the variation of photon absorption rate with depth below the illuminated surface of both the bulk and thin films of Gallium Antimonide (GaSb) semiconductor was determined at different temperatures. Then, the total photon absorption rate in both thin film and bulk semiconductor as a function of the thicknesses for different temperatures is described. The results obtained from the description of photon absorption rate, shows that; temperatures with different absorption coefficients have different absorption rates at a given depths. At depth below the illuminated surface, photon with depths less and greater than the penetration depth of the illumination have negligibly small absorption rates, so that the absorption rate at the absorption depth of a photon is equal to 37% of its maximum absorption rate at the illuminated surface. Temperatures with higher absorption coefficients are absorbed more near the illuminated surface and temperatures with low absorption coefficients are passing through the materials without being absorbed (or with a few absorption effect). Therefore, each point inside a thin film semiconductor has more photon absorption rate as compared to the corresponding points in thick semiconductors. As a result of the reduction in the photon absorption rate occurred in the bulk semiconductor and compensated in thin films due to the multiple reflections of photon from the top and the bottom surfaces into the film semiconductors. The total photon absorption rate in the entire material is also increases with decreasing the thickness of the films. Temperatures with high absorption coefficients are absorbed at high rate and Temperatures with low absorption coefficients are passing unabsorbed (with less absorption) through the materials. The analysis of the band bending of GaSb indicates that, the band bending energy is decreasing at low temperatures than high temperatures at the two surfaces of a thin film semiconductor.

The results of the analysis of the excess carriers lifetime confirms that, the depletion region of the thermal equilibrium majority carrier concentration enhances the magnitude of the low injection level excess carrier lifetime in the under surface depletion layer than in the deep bulk. The magnitude of the radiative excess minority carrier lifetime is highly decreasing in the deep bulk of the semiconductor with decreasing the temperatures from the maximum of the depletion layer width for

temperature 256 K, while the magnitude of the radiative excess minority carrier lifetime under the surface is not able to respond at low temperatures. Since majority carrier Concentration in the depletion layer decreases from maximum value p_0 at the edge of the quasi-neutral region towards the surface, attains its minimum value at the surface. Even though, the radiative excess minority carrier lifetime is increasing and decreasing with increasing the temperatures from the maximum value of the depletion layer width for temperature 256 K for the deep bulk and under the surface of the semiconductor, respectively. The effects of high injection level and low energy photon can be detected equally at all points inside a thin film material, while the effects of the low injection level and low energy photons cannot be detected in the deep bulk, but can be detected under the top and the bottom surfaces. The effects of an illumination with high energy and high injection level can be detected at different points inside a material with various photo responses. However, the effect of an illumination with high energy and low injection level can be detected only under the illuminated surface.

References

[1] L. Łukasiak and A. Jakubowski, "History of semiconductors," *Journal of telecomunications and information technology,* pp. 3-9, 2010.

[2] E. E. Loebner, "Subhistories of the light emitting diode," vol. 23, p. 675–698, 1976.

[3] N. Holonyak, "The semiconductor laser," vol. 85, p. 1678–1693, 1997.

[4] B. K. Ridley, "Large band gap semiconductors," *Tr. j. of physics,* vol. 23, pp. 577-580, 1999.

[5] A. Goswami, "Thin Film Fundamentals," *New Age International pvt ltd,* 2008.

[6] H. R. Jappor, "Band-structure calculations of GaAs within semiempirical large unit Cell method," *European journal of scientific research,* vol. 59, pp. 264-275, 2011.

[7] R. K. Lal, P. Chacrabarti, "Progress in crystal growth and characterization of materials," vol. 52, p. 33, 2006.

[8] M. W. Shura, "Photoconductive spectroscopy of GaSb thin films, PhD thesis, Nelson Mandela Metropolital University,South Africa," 2013.

[9] N. Zia, "Fabrication and characterization of broadband superluminescent diodes for 2μm wavelength," pp. 30-31, 2015.

[10] H. K. Guangyu, C. O. Lupan, L. H. Heinrich, S. P. Schulte, "In-situ boron doping of chemical-bath deposited CdS thin films," vol. 206, no. 2, pp. 256-262, 2009.

[11] D. B. Hard et al, "Thin film on glass," pp. 1-21, 2003.

[12] Z. C. Feng, F. C. Hou, J. B. Webb, Z. X. Shen, E. Rusli, I. T. Ferguson, W. Lu, "Optical investigation of GaSb thin films grown on GaAs by metal organic magnetron sputtering," *Thin solid films,* vol. 516, p. 5493–5497, 2008.

[13] G. Astromskas, M. Jeppsson, P. Caroff, L. Wemersson, “Temperature dependence of GaSb overgrowth of tungsten on GaSb (001) substrates using movpe,” pp. 354-356, 2008.

[14] D. Daspet, F. Espioussas, A. Johan, M. Roux, “High injection effects on conductivity and carrier lifetime in P-type Silicon material,” *Revue de physique appliquee,* vol. 15, pp. 945-959, 1980.

[15] D. K. Schroder, “Carrier lifetimes in silicon,” *IEEE transactions on electron devices,* vol. 44, pp. 160-170, 1997.

[16] S. K. Pang and A. Rohatgi, “Record high recombination lifetime in oxidized magnetic czochralski silicon,” *Applied physics letter,* pp. 195-197, 1991.

[17] M. W. Shura, V. Wagener, J. R. Botha and M. C. Wagener, “Non-linear injection level dependence of the excess carrier lifetime of p-type GaSb thin films: A two-layer model,” *J. appl. phys,* vol. 111, 2012.

[18] G. Mustafa, M. R. I. Chowdhury, D. K. Saha, S. Hussain, and O. Islam, “Annealing effects on the properties of chemically deposited CdS thin films at ambient condition,” vol. 60, no. 2, pp. 283-288, 2012.

[19] H. H. Abu-Safe, H. H. Naseem, W. B. Al-dhafiri, “Chlorine-doped CdS thin films from CdCl2-mixed CdS powder,” *Journal of electronic materials,* vol. 33, no. 2, p. 128–134, 2004.

[20] W. L. Hui and J. P. Corra, “Thin-film Cadmium Sulfide solar cell array,” pp. 86-87, 1966.

[21] B. R. Green, “Hall Effect measurement for Semiconductors and material characterization,” 2011.

[22] M. W. Shura, V. Wagener, J. R. Botha, “photoconduction spectroscopy of p-type GaSb films,” vol. 407, pp. 1656-1659, 2012.

[23] J. A. Owolabi, M. Y. Onimisi, S. G. Abdu, G. O. Olowomofe, "Determination of band structure of Gallium-Arsenide and Aluminium-Arsenide using density functional theory," *Computational chemistry,* vol. 4, pp. 73-82, 2016.

[24] A. Shaheen, W. Zia and M. S. Anwar, "Band structure and electrical conductivity in semiconductors," pp. 1-25, 2010.

[25] K. Schroder, "Semiconductor material and device characterization, New york: John Wiley and Sons," 1998.

[26] M. Buscema, M, Barkelid, V, Zwiller, H. S. J. van der Zant, G. A. Steele, A. Castellanos, "Large and tunable photothermoelectric effect in single-layer MoS2," *Nano letters,* pp. 1-6, 2012.

[27] C. Kittel, "Introduction to solid state physics, Wiley, seventh edition," 2010.

[28] T. R. Harris, "Optical properties of SI, GE, GAAS, GASB, INAS, AND INP at elevated temperatures," pp. 45-47, 2010.

[29] Y. P. Varshni, " Temperature dependence of the energy gap in semiconductors," *Physica,* vol. 34, p. 149, 1967.

[30] F. Hejaz, "Growth and characterization of GaSb grown from a split-sputtering," pp. 17-18, 2014.

[31] I. Vurgaftmana and J. R. Meyer, "Band parameters for III–V compound semiconductors and their alloys," *Journal of applied physics,* vol. 89, pp. 5830-5832, 2001.

[32] J. P. McKelvey, "Solid-State and semiconductor physics 2nd ed., Harper & Row., New York," 1966.

[33] John Wiley & Sons, Inc, C. kittel, "Introductioti to solid state physics," 8th ed 2005.

[34] S. S. Li, "Semiconductor physical electronics springer, New York," 2006.

[35] E. A. Saleh, "Fundamentals of photonics, 2nd edition," 1991.

[36] J. Piotrowski, “Infrared detectors,” *Acta physica Polonica A,* vol. 87, pp. 303-316, 1995.

[37] J. P. Colinge, “Physics of semiconductor devices,” pp. 29-31, 212.

[38] B. G. Streetman and S. K. Banerjee, “Solid state electronic devices, fifth or sixth edition,” 1995.

[39] F. D. Lenahan, “Photoconductivity and minority carrier lifetimein Tin Sulfide and Gallium Arsenide semiconductors for photovoltaics,” pp. 17-18, 2016.

[40] M. W. Shura, V. Wagener, J. R. Botha, M. C. Wagener, “Non-linear injection level dependence of the excess carrier lifetime of p-type GaSb thin films: A two-layer model,” *Journal of applied physics,* vol. 111, pp. 1-7, 2012.

[41] J. F. Roller, “Contactless spectral-dependent measurement of bulk lifetime and surface recombination velocity in silicon photovoltaic materials,” p. 55, 2016.

[42] E. Kioupakis, Q. Yan, D. Steiauf, “Temperature and carrier-density dependence of auger and radiative recombination in nitride optoelectronic devices,” *New journal of physics,* vol. 15, pp. 2-14, 2013.

[43] H. Matsuura, “Calculation of band bending in ferroelectric semiconductor,” *New journal of physics 2,* vol. 2, pp. 8.1- 8.11, 2000.

[44] J. J. Sparkes, “Semiconductor devices, second edition, London,” 1994.

[45] R. H. Bube, “Photoelectronic properties of semiconductors Cambrdge University Press, Lavergne,TN,” 2010.

[46] C. G. B Garret and W. H. Brattain, “Nonavalanche injection of hot carriers into SiO2,” *Phys. Rev,* vol. 99, p. 376, 1955.

[47] J. Geurts, “Surface science reports,” vol. 18, pp. 1-89, 1993.

[48] M. S. Tyagi, “Introduction to semiconductor material and devices John Wiley and Sons, New york,” 1991.

[49] R.K. Lal, P. Chakrabarti, “A comparison of dominant recombination mechanisms in n-type InAsSb materials,” vol. 52, pp. 33-39, 2006.

[50] B. G. Streeman, “ Solid state electronics devices 6th edition Prentice-Hall, Inc, New,” 2006.

[51] F. Bouzid and L. Dehimi, “Performance evaluation of a GaSb thermophotovoltaic converter,” *Revue des energies renouwelables,* vol. 15, pp. 383 - 397, 2012.

[52] A. Rakoviska, X. Markadet, B. Vinter, K. Bouzehoune, D. kaplan, “Optical characterization and room temperature lifetime measurements of high quality MBE-grown InAsSb on GaSb,” *Semicond. Sci. and technol,* vol. 15, p. 34, 2000.

[53] A. Chandola, R. Pino, P. S. Dutta, *Semicond. Sci. Technol,* vol. 20, p. 886, 2005.

[54] A. cuevas and D. Macdonald, “Measuring and interpreting the lifetime of silicon wafers,solar energy,” vol. 76, pp. 257-258, 2003.

[55] W. Lochmann, “Phonon-assisted auger recombination in semiconductors,” *phys status solid,* pp. 2-8, 1997.

[56] S. Ali, “Electron - ion recombination data for plasma applications,” pp. 17-18, 2012.

[57] R. J. kumar, J. M. Borrego, P. S. Dutta, R. J. Gutmann, “Auger and radiative recombination coefficients in 0.55 eV InGaAsSb,” 2004.

[58] W. Van. Roosbroeck and W. Shockley, “Photon - radiative recombination of electrons and holes in Germanium,” *Phys. rev,* vol. 94, p. 1558, 1954.

[59] A. Rogaliski and Z. Orman, “Infrared physics,” vol. 25, p. 551, 1985.

[60] Y. Arafat, F. M. Mohammedy, M. M. Shahidul, “Optical and other measurement techniques of carrier lifetime in semiconductors,” *International journal of optoelectronic engineering,* vol. 2, no. 2, pp. 5-11, 2012.

[61] M. J. Marinella, Member, IEEE, D. K. Schroder, Life Fellow, IEEE, G. Chung, M. J. Loboda, Senior Member, IEEE, Tamara Isaacs-Smith, and J. R. Williams, Member,

IEEE, “Carrier generation lifetimes in 4H-SiC MOS capacitors,” *IEEE transactions on electron devices,* vol. 57, pp. 1910-1923, 2010.

[62] M. Z. Rahman, “Modeling minority carrier’s recombination lifetime of p-Si solar Cell,” *International journal of renewable energy research,* vol. 2, pp. 118-121, 2012.

[63] A. Cuevas, D. Macdonald, “Measuring and interpreting the lifetime of silicon wafers,” vol. 76, p. 255–262, 2004.

[64] J. P. Nerou, A. Filion, P. E. Girard, “Low temperature surface conductivity of GaSb,” *J. Phys,* vol. 9, pp. 479-489, 1975.